MODELING CAVITATION EFFECTS ON LOW SPEED INDUSTRIAL JOURNAL BEARING LUBRICATION

By

Azhar Zeb

MS (Industrial & Manufacturing Engineering)

(2009-NUST-MS-MSE&M-04)

Thesis submitted in partial fulfillment of
the requirements for the degree of Masters

Supervisor

Prof. Dr. Riaz Ahmad Mufti

NATIONAL UNIVERSITY OF SCIENCES AND TECHNOLOGY

SCHOOL OF MECHANICAL AND MANUFACTURING ENGINEERING, ISLAMABAD, PAKISTAN

FORM TH-4

NATIONAL UNIVERSITY OF SCIENCES AND TECHNOLOGY

MASTER THESIS WORK

We hereby recommend that the dissertation prepared under our supervision by: (Student Name & Regn No.) **Mr. AZHAR ZEB & 2009-NUST-MS-MSE&M-04** Titled: "**Modeling Cavitation Effects on Low Speed Industrial Journal Bearing Lubrication"** be accepted in partial fulfillment of the requirements for the award of **MS** degree with Grade _____.

Examination Committee Members

1. Name:

   Prof. Dr. Abdul Ghafoor Signature:_____

2. Name:

   Asst. Prof. Dr. Liaqat Ali Signature:_____

3. Name:

   Prof. Dr. Muhammad Afzaal Malik Signature:_____

Supervisor's Name:

Prof. Dr. Riaz Ahmad Mufti Signature:_____

_____ _____

Head of Department Date

COUNTERSINGED

Date:_____

_____

Dean/Principal

Modeling Cavitation Effects on Low Speed Industrial Journal Bearing Lubrication

By

Azhar Zeb

Submitted to the Faculty of the School of Mechanical and Manufacturing Engineering, National University of Sciences and Technology, Islamabad, Pakistan, in partial fulfillment of the requirement for the degree of Master of Science in Industrial and Manufacturing Engineering

Candidate:

_____

Azhar Zeb

Advisor:

_____

Prof. Dr. Riaz Ahmad Mufti

Committee Member:

a. Prof. Dr. Abdul Ghafoor

b. Asst. Prof. Dr. Liaqat Ali

c. Prof Dr. Muhammad Afzaal Malik

National University of Science and Technology
School of Mechanical and Manufacturing Engineering

23rd September 2013, Islamabad

PROPOSED CERTIFICATE OF PLAGIARISM

It is certified that MS Thesis Titles, "**Modeling Cavitation Effects on Low Speed Industrial Journal Bearing Lubrication"**, by **"Mr. Azhar Zeb"**, has been examined by us. We undertake the follows:

a. Thesis has significant new work/knowledge as compare already published or are under consideration to be published elsewhere. No sentence, equation, diagram, table, paragraph or section has been copied verbatim from previous work unless it is placed under quotation marks and duly referenced.
b. The work presented is original and own work of the author (i.e. there is no plagiarism). No ideas, processes, results, or words of others have been presented as Author own work.
c. There is no fabrication of data or results which have been compiled/analyzed.
d. There is no falsification by manipulating research materials equipment, or processes, or changing or omitting data or results such that the research is not accurately represented in the research record.
e. The thesis has been checked using TURNITN (copy of originality report attached) and found within limits as per HEC Plagiarism Policy and instructions issued from time to time.

Dated: _____

(Prof. Dr. Riaz Ahmad Mufti)
Supervisor

ABSTRACT

An effective lubrication of journal bearings is jeopardized due to the formation and activity of air cavities in the lubricant. Cavitation affects the buildup of hydrodynamic pressures adversely & lowers the hydrodynamic load carrying capacity of journal bearing. The cavitation effects are quite pronounced for varying speed and eccentricity ratios of journal bearing. In an extreme case, cavitation may cause wear and seizure of the journal bearing. This work will model the cavitation phenomenon and its effects on the journal bearing lubrication numerically using Universal Cavitation Algorithm leading to a single Reynolds equation which is valid for both the full film (liquid) and cavitation zones. The parametric study at commercially available different lubricating oils for varying eccentricity ratios of the journal to bush radial clearances will be conducted for optimization under the stated cavitation conditions for an in-depth analysis for the logical conclusions.

ACKNOWLEDGMENT

First and foremost, I would like to thank the Allah Almighty, Who gave me courage, capability, resources and opportunity to undertake this research work.

My time at SMME (NUST) is personally and professionally rewarding due to support and friendship of many people.

I would like to thank my advisor Prof. Dr. Riaz Ahmad Mufti, for his guidance and support for the completion of my research work. I would also like to thank to Assoc. Prof Dr. Liaqat Ali for his countless support for the completion of my dissertation. I am also thankful to Prof. Dr. Muhammad Afzaal Malik (Air University) for his professional, technical competence and never ending encouragement for the guidance of my research work. Also, I would like to thank principal of SMME (NUST) Prof. Dr. Abdul Ghafoor for his vision & leadership skills to conceive & successfully run MS programme at SMME (NUST).

Particularly, I would like to pay very special tribute to Dr. Syed Adnan Qasim for not only motivating me to undertake this research but also providing continuous guidance and support throughout my thesis work. I would also like to pay thanks to his Mrs. for bearing me for research work in the drawing room of Dr. Adnan's House.

I have been fortunate to met and work with many wonderful fellows like Mr. Mumtaz Ali Khan, Mr. Usman Farooq, Mr. Ali Usman, Mr. Muhammad Saif ullah Khaild, Mr. Mubashir Gulzar, Mr. Rashid Naseer, Mr. Shoaib Ansari, Mr. Azhar Mehmood, Mr. Zahid ullah and Mr. Fakhar-e-Alam Khan who made my time during studies at SMME (NUST) enjoyable and whose continuous help and encouragement made it possible for me to reach all the way at this point.

I would like to thank my beloved parents, who always guided me in the right way and whose endless effort and support made it possible for me, to be, what I am today.

I would like to thank my wife, for her countless encouragement and sparing me for the completion of my research work.

In the end, I would like to thank the entire honorable faculty of SMME (NUST), whose professional approach, dedication and hard work made all this possible for me.

Azhar Zeb
23rd September, 2013

TABLE OF CONTENTS

TABLE OF FIGURES

1. INTRODUCTION

Beauchamp Tower, an engineer by profession, at the end of the nineteenth century noticed serious understanding of hydrodynamics in lubrication when he noticed that the oil in a journal bearing leaked out of a hole located underneath the load. The oil leakage created so much nuisance that he plugged the hole with a cork, however, oil still managed to ooze out. He then plugged the hole with a hard wooden bung. The original idea of provision of hole at bearing was to allow oil supply into the bearing for its lubrication. Later Mr. Tower made it realized that some unknown mechanism was forcing the oil to get pressurized and that mechanism pushed the hard wooden bung out of the oil supply hole as well. Inspired by the human instinct of inquisitiveness Mr. Tower measured the oil pressure and revealed that a hydraulic force could separate the sliding surfaces [2].

During that era of late nineteenth century, Sir Osborne Reynolds and other theoreticians were working on the theory of hydrodynamic lubrication and Beauchamp Tower's discovery alongwith its detailed data provided the experimental evidence of hydrodynamic lubrication given by Sir Reynolds. Later in 1886, theory of hydrodynamic lubrication was published in the Proceedings of the Royal Society London [3].

Sir Osborne Reynolds analytically proved first time in the history of mankind in his famous research published at Royal Society of London in 1886 that two sliding surfaces can be physically separated by hydrodynamic pressure of a viscous liquid within the surfaces which also resulted in less friction and zero wear theoretically.

Osborne Reynolds in his landmark paper of 1886 investigated the case of two cylindrical bearing surfaces operating eccentrically with respect to each other. In his same classical paper, he also clearly accepted the possible influence of ***cavitation*** in lubricant films on bearing behavior. The cavities formation and their manifestation clearly affect the hydrodynamic pressure generated within a lubricant’s continuous thin film, resulting compromise of journal bearings operational performance and reliability.

1.1. JOURNAL BEARING

Journal bearing is very common engineering component. It is used in almost every type of engineering machinery. Efficiency and reliability of rotary equipment like IC engines, pumps, compressors, turbines & generators mainly depend on journal bearings. Journal bearing has a shaft rotating within a stationary bush. The lubricant film help support the load by the generation of hydrodynamic pressure generated by the moving shaft within the bush of the bearing [4].

Figure 1-1 : Journal Bearing (adapted from [1])

Analysis of journal bearing has two basic aspects. The first aspect covers the basic analysis of its load carrying capacity, friction generated between moving surfaces and lubricant flow rate as a function of speed, load and any other controlling parameters [4]. The second aspect covers the practical issues with its operation, which include its design improvement to suppress cavitation and vibration, lubricant supply methodology, degree of misalignment to accommodate fit for its operation, and heating of introduced lubricant due to friction [4].

1.2. BEARING GEOMETRY

Journal bearing's geometry is shown at figure: 1-2 below:

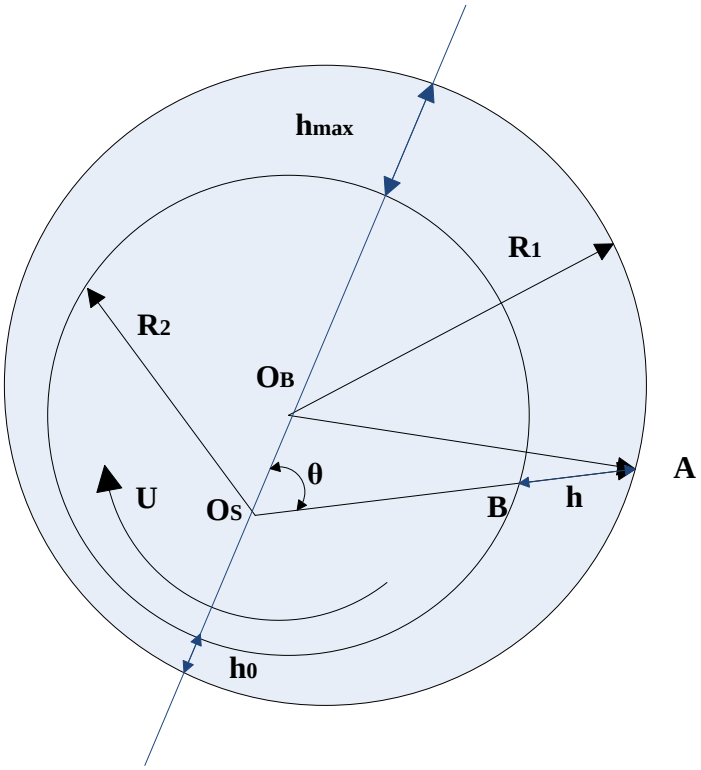

Figure 1-2 : Geometry of the journal bearing (adapted from [4]).

Where
R_1 = Radius of the bush,
R_2 = Radius of the shaft,
O_B = Centre of the bush,
Os = Centre of the shaft.

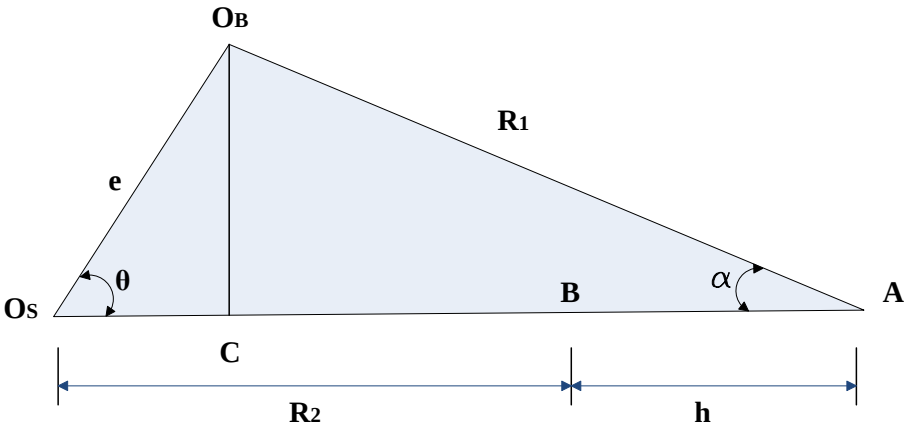

Figure 1-3 : Geometry detail of lubricant film shape in journal bearings (adapted from [4]).

Where:

e = Eccentricity (distance OsOB between the axial centres of shaft and bush during bearing's operation)

h = Lubricant film thickness.

Consider ΔOsO_BA from figure-1.2 which is shown in detail at figure: 1-3. It should be noted that the angle 'α' is very small. From inspection of the triangle ΔOsO_BA it can be written:

$$O_s A = O_s C + CA = O_s B + BA$$
$$or \qquad \text{---------- (Eq:1.1) [4]}$$
$$O_s A = e\cos\theta + R_1\cos\alpha = R_2 + h$$

thus:

$$h = e\cos\theta + R_1\cos\alpha - R_2 \text{ ---------- (Eq:1.2) [4]}$$

Making use of sine rule we get

$$\frac{e}{\sin\alpha} = \frac{R_1}{\sin\theta}$$
$$\Rightarrow \sin\alpha = \frac{e}{R_1}\sin\theta \qquad \text{---------- (Eq:1.3) [4]}$$

As

$$\sin^2\alpha + \cos^2\alpha = 1 \text{ ---------- (Eq:1.4) [4]}$$

Making use of $\sin\alpha$ yields:

$$\cos\alpha = \sqrt{1-\sin^2\alpha} = \sqrt{1-\left(\frac{e}{R_1}\right)^2\sin^2\theta} \text{ ---------- (Eq:1.5) [4]}$$

Since $\frac{e}{R_1} << 1$ then:

$$\cos\alpha \approx 1 \text{ ---------- (Eq:1.6) [4]}$$

Making use of above in eq (1.1) yields:

$$"h = e\cos\theta + R_1 - R_2 = e\cos\theta + c" \text{ ---------- (Eq:1.7) [4]}$$

Where $c = R_1 - R_2$=Clearance (Difference between Radii of shaft & bush [4].

or:

$$"h = c(1+\varepsilon\cos\theta)" \text{ ---------- (Eq:1.8) [4]}$$

Where ε, is eccentricity ratio [4]

$$"\varepsilon = \frac{e}{c}"$$ ---------- (Eq:1.9) [4]

Equation (1.3) gives a description of film shape in journal bearings with an accuracy of 0.1% [4, 5].

1.3. PRACTICAL AND OPERATIONAL ASPECTS OF JOURNAL BEARING

Nowadays journal bearings are designed for a number of rotary machinery with varying requirements of design as per their operational requirements. Due to variety of design requirements there are some issues associated with the operation and their practical implementation for journal bearings. For example, in many applications the lubricating oil is usually fed under pressure, for that reason some critical shaft speeds to be avoided due to resonance frequencies of the bearing [4]. In order to insert shaft as per its fits requirement, a tolerance is usually specified as per Hole Basis or Shaft Basis System. So the shaft is usually misaligned i.e. eccentric and there are always some effects of ***cavitation*** of lubricating films. And elastic deformation of the bearing surfaces will certainly happen. All of these issues affect the reliability and performance of a journal bearing to some level so allowance should be made during the design and operation of the journal bearing.

1.4. CAVITATION

In stationary situation, cavitation of liquid occurs if its pressure falls below its vapour pressure at that temperature. In a dynamic and transient condition, the pressure may fall significantly below the vapor pressure and may be even lower than the vacuum pressure. In the latter scenario, surface tension generated within the fluid [6] before the film ruptures and starts cavitation. As this phenomenon is of the transient nature and has its negligible effect on its steady-state condition, so null pressure gradient or a constant pressure value is the boundary conditions specified for the cavitated region [5].

According to Young, Cavitation is the formation and activity of bubbles (or cavities) in a liquid and is of four different kinds [7].

a. Hydrodynamic Cavitation

Hydrodynamic cavitation is produced by pressure variations in a flowing liquid due to the geometry of the system [7].

b. Acoustic Cavitation

Acoustic Cavitation is produced by sound waves in a liquid due to pressure variations [7].

c. Optic Cavitation

Optic Cavitation is produced by photons of high intensity (laser) light rupturing in a liquid [7].

d. Particle cavitation

Particle cavitation is produced by any other type of elementary particles, e.g. a proton, rupturing as in a bubble chamber [7].

Hydrodynamic liquid cavitation has three recognized forms as follows [8].

a. Gaseous cavitation

Gaseous cavitation usually occurs when pressure of one or more dissolved gases falls below its saturation pressure in the liquid [8].

b. Pseudo-cavitation

Pseudo-cavitation is a form of gaseous cavitation during which the gas bubble expands on account of depressurization without further gas mass diffusion from the liquid to the gas phase [8].

c. Vaporous cavitation

Vaporous cavitation is the result of a thermodynamic non-equilibrium event when the pressure falls below the vapour pressure [8].

2. LITERATURE REVIEW

2.1 INTRODUCTION

Literature review on cavitation in thin liquid films in bearings couldn't be completed if we miss three symposia held on cavitation. Such first symposium in modern age was organized by General Motors Research Labs in 1962 [8, 9], which is organized by and edited by Davies. This was the first ever symposium held about cavitation at one place and many of its participants are today considered as forefathers in developing knowledge about bubble dynamics [10, 11], surface tension [12, 13] and thin film rupture [8, 14-16] .

The second such symposium was held in 1974 as 1st Leeds-Lyon Symposium, edited by Dowson et al. [17], was the first in history to focus singly on cavitation phenomena related to lubrication technology [8]. Its report contains information about the fundamentals of vaporous and gaseous cavitation and classical theories were presented to address film rupture conditions in static and dynamically loaded bearings alongwith the research related to cavitation damage as well [8].

The third symposium regarding cavitating films was held in 1988 at NASA Lewis Research Center (Cleveland, Ohio, USA), Brewe et al. [18] edited the most recent advances and the improved version of models were presented for basic fundamental concepts of cavitation already presented in 1974 at Lyon [8, 17]. The 1988 symposium offered novel theoretical algorithms in particular for a more realistic simulation and numerical implementation of lubricant film cavitation problems [8].

2.2 FILM RUPTURE THEORIES

Cavitation, a rupture in the continuity of the liquid film either comes from the lubricating film (in case of gaseous cavitation) or from the environment (in case of vaporous cavitation) [8]. Researchers faced a huge challenge in the context of the solution to the Reynolds equation due to this discontinuity at the bubble interface. Sommerfeld [19] did not take into account film rupture and didn't solve for a full film around the circumference as shown in figure: 2-1 [8].

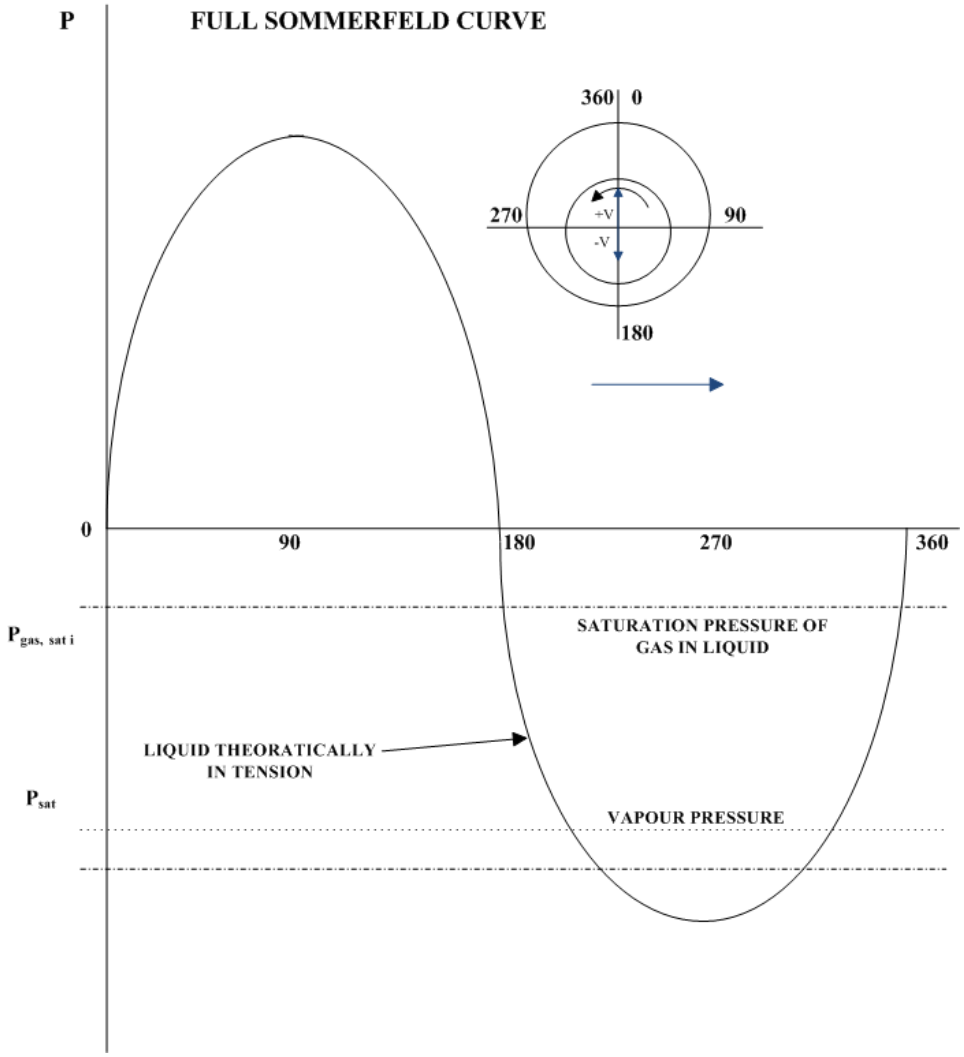

Figure 2-1 : Typical pressure distribution in a journal bearing with an eccentric shaft: 2D full Sommerfeld curve circumferential cross section through the symmetry line of pressure distribution in a convergent–divergent clearance with a normal velocity ±V to the main flow direction (adapted from [8]).

In 1914 Gumbel [20] was the first to consider for the film 'rupture'. According to him, "for a steadily loaded bearing operating at constant angular velocity, the rupture originates in the immediate vicinity of the film's minimum clearance, at a predetermined pressure P_{cav} and remains constant at that value for the entire divergent region [8]" as shown in figure-2.1. Film reformation and mass continuity was not considered in his approach [8]. As the circumferential pressure distribution allows only the convergent film zone, i.e. positive pressure region, so the Gumbel condition is also known as the 'half-Sommerfeld' condition figure: 2-2(a) [8].

Gumbel's condition represents an early simplistic approach that only that recognized the physical reality of the film rupture and basis for an analytical and numerical simulation [8]. Later, a better alternative to the 'half-Sommerfeld' condition was offered by two researchers Swift [21] and Stieber [22] independently of each other as shown at figure: 2-2(a) [8]. In 1932 Swift [21] described that a zero derivative of the pressure is a suitable condition for onset of cavitation and called it to be a 'stability condition' [8]. In 1933 Stieber [22] published a full solution for a 360 degree journal bearing considering cavitation [8]. This solution was done for a zero tensile strength lubricant. Later Floberg adapted the different approaches for the zero and non-zero tensile stress for the cavitation of lubricant film [8, 23].

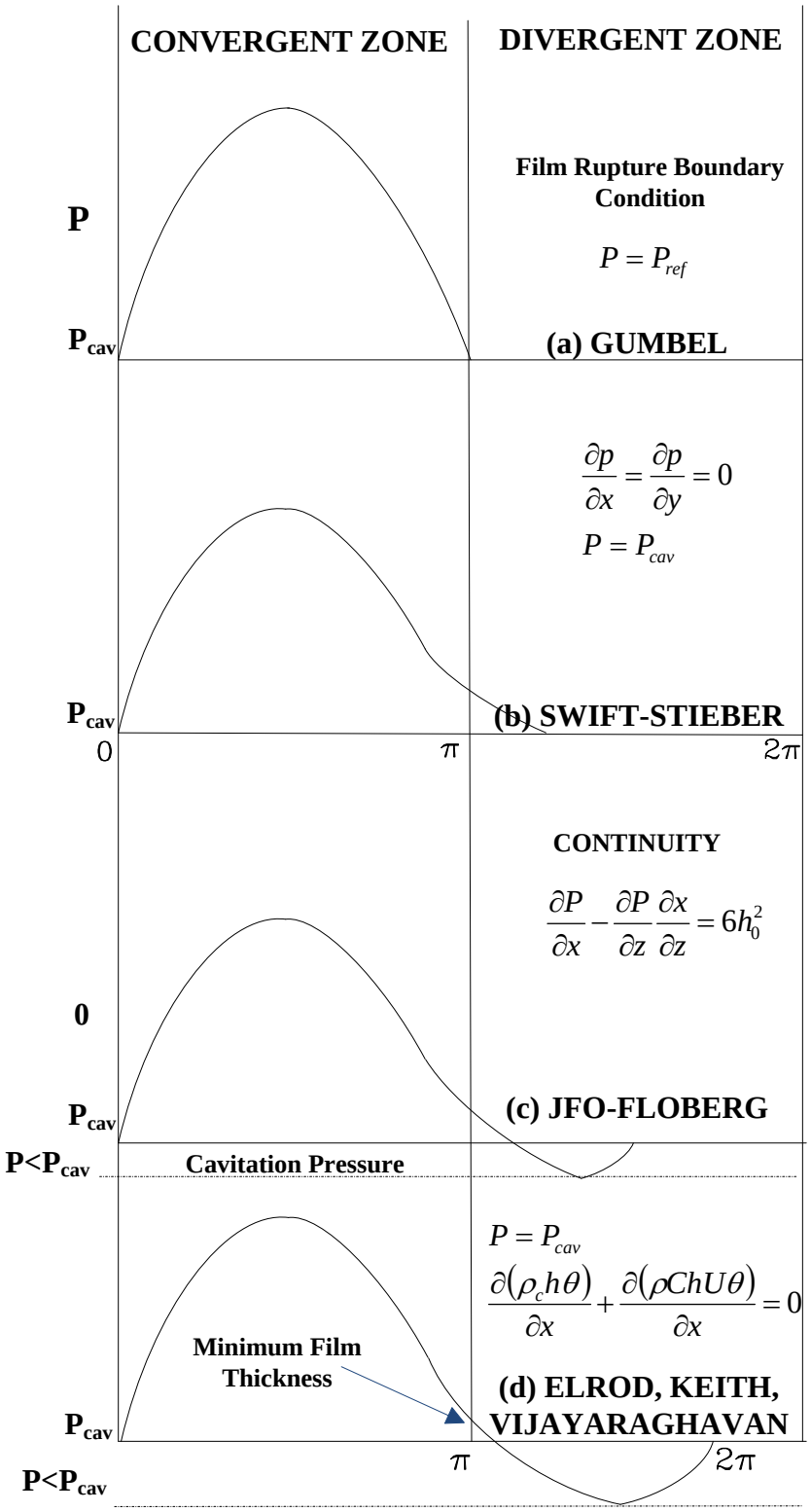

Figure 2-2 : Circumferential pressure development based on film rupture theories: (a) Gumbel [20]; (b) Swift–Stieber [21, 22]; (c) JFO and Floberg; and (d) Elrod [24], and Vijayaraghavan and Keith [25, 26] (adapted from [8])

Stieber, like Swift considered continuity condition as a zero-pressure gradient at the start of the cavitation zone. Both while approaching it from different angles came to the same conclusion regarding its inception and development. These cavitation zone formation conditions are now famous as the Swift–Stieber conditions as shown at figure: 2-2(b) are:

$$"\frac{\partial p}{\partial x} = \frac{\partial p}{\partial y} = 0"\&"P = P_{cav}" \text{ ---------- (Eq:2.1)[8]}$$

The above conditions consider the whole cavitation zone at $P = P_{cav}$ and do not allow for the existence of sub-cavitational or variations in the pressure inside the cavitation region [8]. After the rupture of film, Poiseuille (flow between the plates due to pressure difference across their separation) flow component of the circumferential and axial velocities becomes zero, and only the Couette (flow between two parallel plates, caused by relative motion of the plates) flow component is sole responsible for carrying lubricant in between the gas cavities as shown in figure: 2-3 [8].

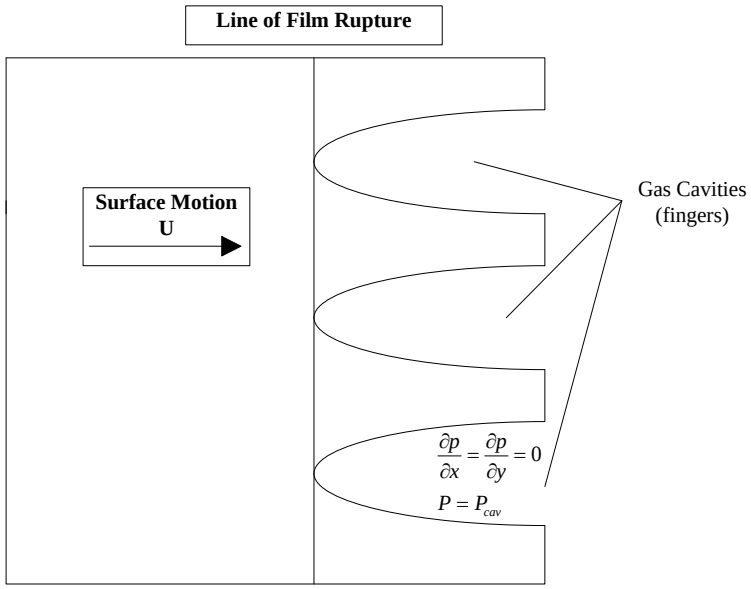

Figure 2-3 : Film rupture boundary conditions type-striated gas and liquid fingers (Swift Stieber, JFO)

As null pressure gradient is imposed within the cavitation region by setting a constant pressure of lubricant so the pressure gradient calculated within the lubricant has to interface with the cavity pressure gradient along the boundary in such a way that at certain locations there can be a relatively steep slope (e.g. the point of cavity inception) [8].

3. REYNOLDS EQUATION

3.1 INTRODUCTION

In 1886, Sir Osborne Reynolds gave the basis of lubricating film theory and proved with his famous experiment of rotating cylinders with olive oil between them as lubricant and explained how a viscous liquid can physically separate two sliding surfaces by built up of lubricant's hydrodynamic pressure which resulted in low friction and negligible wear [4]. This theory became the basis for the mechanism of lubrication by the generation of a viscous liquid film between the sliding surfaces [4]. Lubricant between two sliding surfaces provides the load carrying capability when first surface is being inclined to the second at a certain angle and other moves relatively to the first with an certain velocity. Reynolds equation can be a simplified version of the Navier-Stokes momentum and continuity equation by neglecting inertia and body forces. Or, this equation can also be derived by applying the continuity of flow principle by considering the continuity of flow in a column subjected to viscous shear. Reynolds equation is very useful in determining hydrodynamic pressures generated between rigid moving surfaces [4].

3.2 PRINCIPLE OF HYDRODYNAMIC PRESSURE GENERATION

Principle of hydrodynamic pressure generation between moving non-parallel surfaces is schematically illustrated at figure: 3-1.

Following assumptions are made to apply this principle [4]:-

The bottom surface, here it is called as the 'runner', moves with a certain velocity and is covered with lubricant. The top surface is set to be inclined at a specific angle to the bottom surface. The bottom surface drags the lubricant alongwith it into the converging wedge as it moves along. Doing so, the bottom surface generates a pressure field else entering lubricant would be more than leaving the wedge. So the increase in lubricant pressure restricts the flow at entry point of the wedge and there is a decrease in pressure boosting the exit flow at the exit. This makes a positive pressure gradient which makes the fluid velocity profile to bend inwards at the entry

to the wedge and bend outwards at the exit of the wedge, as shown in the figure: 3-1. Thus the pressure generated physically separates the two surfaces and helps support a specific load. If a curved shape wedge is wrapped around a shaft then it forms a typical engineering application called as journal bearing [4].

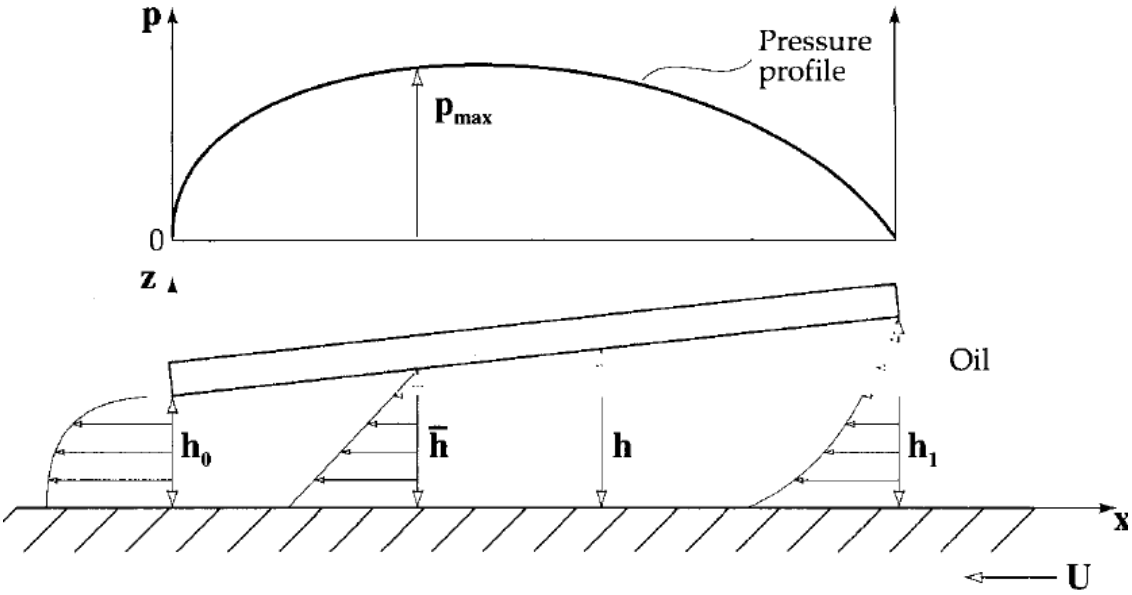

Figure 3-1 : Principle of hydrodynamic pressure generation between non-parallel surfaces (adapted from [4])

Table-3.1 : Summary of simplifying assumptions in hydrodynamics (adapted from [4])

S#	Assumption
1	Body forces are neglected
2	Pressure is constant through the film
3	No slip at the boundaries
4	Lubricant behaves as a Newtonian fluid
5	Flow is laminar
6	Fluid inertia is neglected
7	Fluid density is constant
8	Viscosity is constant throughout the generated fluid film

3.3 DERIVATION OF REYNOLDS EQUATION

In order to obtain expression of fluid particles and continuity of flow in a column Let us consider the equilibrium of a fluid element as shown in figure: 3-2 [4].

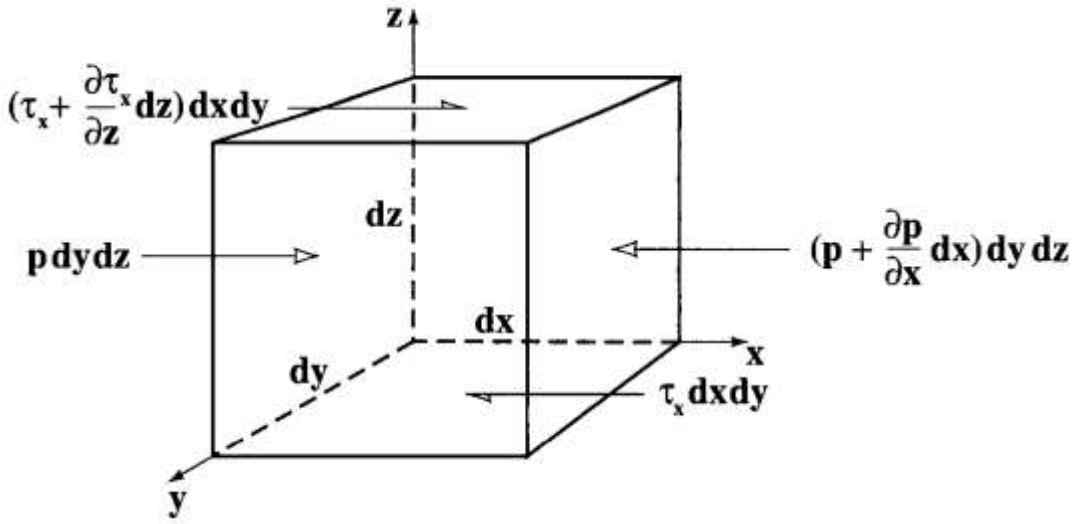

Figure 3-2 : Equilibrium of an element of fluid from a hydrodynamic film; p is the pressure, τ_x is the shear stress acting in the 'x' direction.

Consider a small element of fluid from a hydrodynamic film [4]. Assume that forces acting on the element are acting in the x-direction only [4]. Since element is in equilibrium hence forces at the left balance the forces at the right [4]. Mathematically, it is given by

$$" pdydz + (\tau_x + \frac{\partial \tau_x}{\partial z} dz)dxdy = (p + \frac{\partial p}{\partial x} dx)dydz + \tau_x dxdy"$$ ---------- (Eq:3.1) [4]

Simplifying, yields

$$"\frac{\partial \tau_x}{\partial z} dxdydz = \frac{\partial p}{\partial x} dxdydz"$$ ---------- (Eq:3.2) [4]

Assume that volume is non-zero i.e., $"dxdydz \neq 0"$ [4]

$$"\frac{\partial \tau_x}{\partial z} = \frac{\partial p}{\partial x}"$$ ---------- (Eq:3.3) [4]

Similarly forces acting in ‘y’ direction yield the second equilibrium [4],

$$"\frac{\partial \tau_y}{\partial z} = \frac{\partial p}{\partial y}"$$ ---------- (Eq:3.4) [4]

Applying assumption # 2 from Table-3.1, i.e. pressure is constant through the film [4]. Hence,

$$\frac{\partial p}{\partial z} = 0$$ ---------- (Eq:3.5) [4]

Shear stress can be expressed in terms of dynamic viscosity and shear rate, which is given as [4]

So shear stress acting in the ‘x’ direction

$$"\tau_x = \eta \frac{u}{h} = \eta \frac{\partial u}{\partial z}"$$ ---------- (Eq:3.6) [4]

And shear stress acting in the ‘y’ direction

$$"\tau_y = \eta \frac{v}{h} = \eta \frac{\partial v}{\partial z}"$$ ---------- (Eq:3.7) [4]

Putting equation (3.6) into equation (3.3) yields

$$"\frac{\partial}{\partial z}\left[\eta \frac{\partial u}{\partial z}\right] = \frac{\partial p}{\partial x}"$$ ---------- (Eq:3.8) [4]

Putting equation (3.7) into equation (3.4) yields

$$"\frac{\partial}{\partial z}\left[\eta \frac{\partial v}{\partial z}\right] = \frac{\partial p}{\partial y}"$$ ---------- (Eq:3.9) [4]

Applying assumption # 8 from Table-3.1, i.e. viscosity is assumed to be constant throughout the film. So it is not a function of ‘z’ i.e. $\eta \neq f(z)$

Equation (3.8) can be rearranged as follows by separating the variables yields

$$"\frac{\partial p}{\partial x}\partial z = \partial\left[\eta\frac{\partial u}{\partial z}\right]" \text{ [4]}$$

Integrating both sides

$$"\frac{\partial p}{\partial x}\int \partial z = \partial\int\left[\eta\frac{\partial u}{\partial z}\right]"$$

$$"\frac{\partial p}{\partial x}z + c_1 = \eta\frac{\partial u}{\partial z}"$$

Separating variables again yields

$$"(\frac{\partial p}{\partial x}z + c_1)\partial z = \eta\partial u"$$

Integrate it again yields

$$"\int\left(\frac{\partial p}{\partial x}z + c_1\right)\partial z = \eta\int \partial u"$$

$$"\frac{\partial p}{\partial x}\left(\frac{z^2}{2}\right) + c_1 z + c_2 = \eta u" \text{ ---------- (Eq:3.10) [4]}$$

3.3.1 Defining Boundary Conditions

Keeping in view the assumption that there is no slip or velocity discontinuity between the liquid and solid at the boundaries of the wedge (assumption # 3 from Table-3.1 i.e. velocity of the oil layer adjacent to the boundary is the same as that of the boundary), the boundary conditions are defined as

"$u = U_2$ at $z = 0$"

"$u = U_1$ at $z = h$"

Applying $u = U_2$ at $z = 0$ in equation (3.10) yields

$$"\frac{\partial p}{\partial x}\left(\frac{(0)^2}{2}\right)+(c_1\times 0)+c_2=\eta U_2"$$

"$C_2 = \eta U_2$"---------- (Eq:3.11) [4]

Applying equation (3.11) and u = U_1 at z = h in equation (3.10) yields

$$"\frac{\partial p}{\partial x}(\frac{h^2}{2})+C_1h+\eta U_2=\eta U_1"$$

$$"C_1h+\frac{\partial p}{\partial x}\frac{h^2}{2}=\eta U_1-\eta U_2"$$

$$"C_1+\left(\frac{\partial p}{\partial x}\frac{h^2}{2}\frac{1}{h}\right)=\frac{\eta}{h}(U_1-U_2)"$$

$$"C_1=(U_1-U_2)\frac{\eta}{h}-\frac{\partial p}{\partial x}\frac{h}{2}"$$---------- (Eq:3.12) [4]

Putting equations (3.11) and (3.12) in equation (3.10) yields

$$"\frac{\partial p}{\partial x}\left(\frac{z^2}{2}\right)+\left[(U_1-U_2)\frac{\eta}{h}-\frac{\partial p}{\partial x}\frac{h}{2}\right]z+\eta U_2=\eta u"$$

$$"u=\frac{\partial p}{\partial x}\frac{z^2}{2\eta}+(U_1-U_2)\frac{z}{h}-\frac{\partial p}{\partial x}\frac{zh}{2\eta}+U_2"$$

$$"u=\frac{\partial p}{\partial x}\left[\frac{z^2-zh}{2\eta}\right]+(U_1-U_2)\frac{z}{h}+U_2"$$---------- (Eq:3.13) [4]

Equation (3.13) is the required expression for velocity in the 'x' direction. Velocity profiles at the entry of the hydrodynamic film are shown in figure-3.3 below:

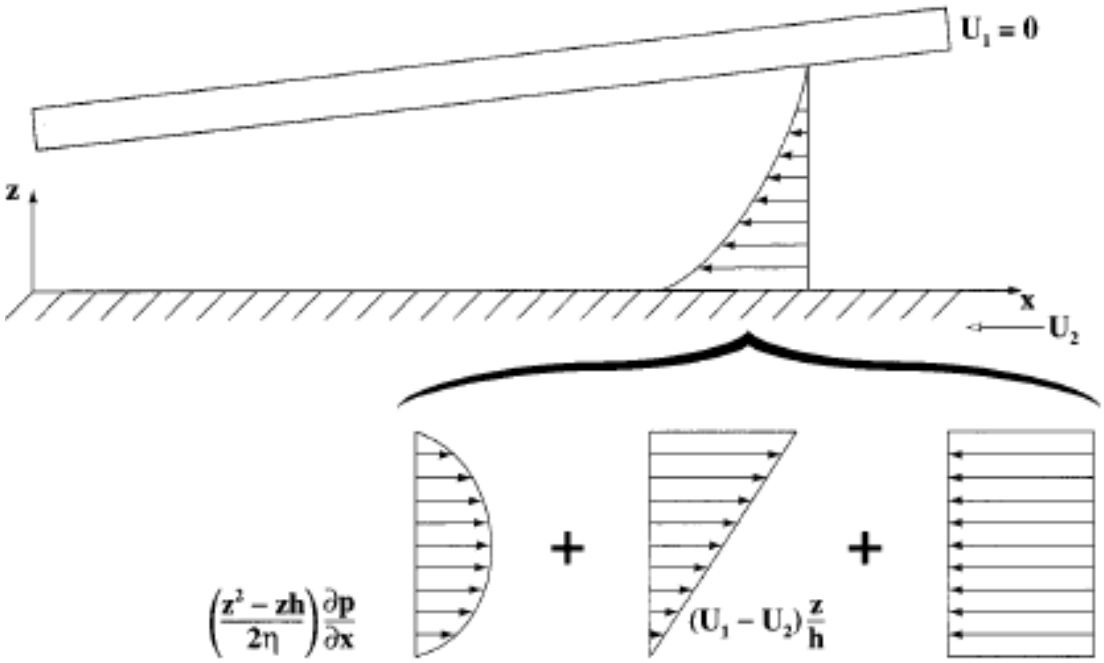

Figure 3-3 : Velocity profiles at the entry of the hydrodynamic film.(adapted from [4])

Applying assumption # 8, i.e. dynamic viscosity is assumed constant. Hence it is not a function of 'z' i.e., $\eta \neq f(z)$. Equation (3.9) can be re-arranged as:

$$"\partial\left(\eta\frac{\partial v}{\partial z}\right)=\left(\frac{\partial p}{\partial y}\right)\partial z"$$

Integrating above will yield

$$"\eta\frac{\partial v}{\partial z}=\frac{\partial p}{\partial y}z+C_1"$$

$$"\eta\ \partial v=\left(\frac{\partial p}{\partial y}z+C_1\right)\partial z"$$

Integrating it again,

$$"\int \eta dv=\int\left(\frac{\partial p}{\partial y}z+C_1\right)\partial z"$$

$$"\eta v=\frac{\partial p}{\partial y}\left(\frac{z^2}{2}\right)+C_1z+C_2"$$ ---------- (Eq:3.14) [4]

In a similar manner a formula for velocity in the 'y' direction is obtained as

$$"v=\frac{\partial p}{\partial y}\left[\frac{z^2-zh}{2\eta}\right]+(V_1-V_2)\frac{z}{h}+V_2"$$ ---------- (Eq:3.15) [4]

3.3.2 Continuity of Flow in a Column

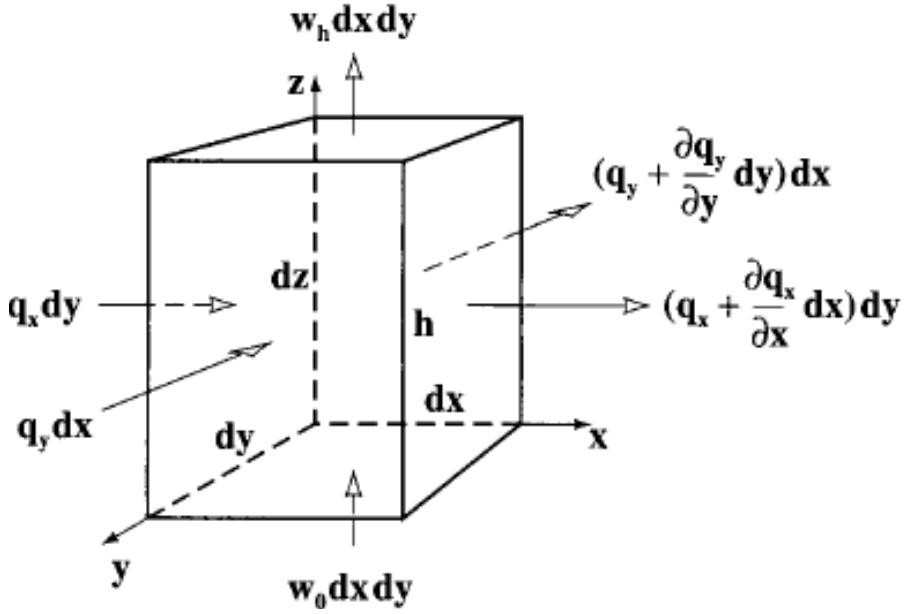

Figure 3-4 : Continuity of flow in a column (adapted from [4])

Consider a column of lubricant as shown in figure-3.4, such that the lubricant flows into the column horizontally at the rates of q_x and q_y [4]. In the vertical direction the lubricant flows into the column at the rate of $w_0 dxdy$ and flows out at the rate of $w_h dxdy$ [4]. The principle of continuity of flow requires that "the influx of a liquid must equal it's efflux from a control volume under steady conditions" [4]. Keeping in view the requirements of this principle and assuming the density of the lubricant to be constant, the following relation applies [4]

$$q_x dy + q_y dx + w_0 dxdy = \left(q_x + \frac{\partial q_x}{\partial x} dx \right) dy + \left(q_y + \frac{\partial q_y}{\partial y} dy \right) dx + w_h dxdy \text{ -(Eq:3.16) [4]}$$

$$"q_x dy + q_y dx + w_0 dxdy = q_x dy + \frac{\partial q_x}{\partial x} dxdy + q_y dx + \frac{\partial q_y}{\partial y} dydx + w_h dxdy" \text{ [4]}$$

$$"\frac{\partial q_x}{\partial x} dxdy + \frac{\partial q_y}{\partial y} dxdy + (w_h - w_0) dxdy = 0" \text{ ---------- (Eq:3.17) [4]}$$

As $dxdy \neq 0$ [4]

equation: 3.17 can be rewritten as

$$"\frac{\partial q_x}{\partial x}+\frac{\partial q_y}{\partial y}+\left(w_h-w_0\right)=0"$$ ---------- (Eq:3.18) [4]

Flow rates per unit length (q_x & q_y) can be found by integrating the lubricant viscosity profile over its film thickness [4]:

$$"q_x=\int_0^h u dz"$$ ---------- (Eq:3.19) [4]

$$"q_y=\int_0^h v dz"$$ ---------- (Eq:3.20) [4]

Putting 'u' in equation (3.13) yields

$$"q_x=\int_0^h\left[\frac{\partial p}{\partial x}\left(\frac{z^2-zh}{2\eta}\right)+\left(U_1-U_2\right)\frac{z}{h}+U_2\right]dz"$$ [4]

$$"q_x=\left|\left(\frac{z^3}{3}\frac{z^2h}{2}\right)\frac{\partial p}{\partial x}\left(\frac{1}{2\eta}\right)\right|_0^h+\left|\left(U_1-U_2\right)\frac{z^2}{2h}\right|_0^h+\left|U_2z\right|_o^h"$$ [4]

$$"q_x=\left(\frac{h^3}{3}-\frac{h^3}{2}\right)\frac{\partial p}{\partial x}\left(\frac{1}{2\eta}\right)+\left(U_1-U_2\right)\frac{h^2}{2h}+U_2h"$$ [4]

$$"q_x=-\frac{h^3}{6}\frac{\partial p}{\partial x}\left(\frac{1}{2\eta}\right)+h\left[\left(\frac{U_1-U_2}{2}\right)+U_2\right]"$$ [4]

$$"q_x=-\left[\frac{-h^3}{12\eta}\frac{\partial p}{\partial x}\right]+\frac{h}{2}+\left(U_1+U_2\right)"$$ ---------- (Eq:3.21) [4]

which is the required flow rate per unit length in the 'x' direction

Now putting value of 'v' from equation (3.15) into equation (3.20) & get

$$"q_y=\frac{-h^3}{12\eta}\frac{\partial p}{\partial y}+\frac{h}{2}(V_1+V_2)"$$ ---------- (Eq:3.22) [4]

which is the required flow rate per unit length in the 'y' direction.

Now putting equations (3.21) & (3.22) into equation (3.18), we get

$$\frac{\partial}{\partial x}\left[-\frac{h^3}{12\eta}\frac{\partial p}{\partial x}+\frac{h}{2}(U_1+U_2)\right]+\frac{\partial}{\partial y}\left[-\frac{h^3}{12\eta}\frac{\partial p}{\partial y}+\frac{h}{2}(V_1+V_2)\right]+(w_h-w_0)=0$$

(Eq:3.22) [4]

In order to simplify the expression for the equation of continuity of flow in a column, we define lubricant velocities in the 'x' and 'y' directions as follows:

"$U = U_1+U_2$" ;"$V = V_1+V_2$"

Assume that there is no local variation in surface velocity in the 'x' and 'y' directions, i.e. "$U \neq f(x)$" & "$V \neq f(y)$"

Apply the above simplification and assumption in equation (3.23)

$$-\frac{\partial}{\partial x}\left[\frac{h^3}{12\eta}\frac{\partial p}{\partial x}\right]+\frac{U}{2}\frac{dh}{dx}-\frac{\partial}{\partial y}\left[\frac{h^3}{12\eta}\frac{\partial p}{\partial y}\right]+\frac{V}{2}\frac{dh}{dy}+(w_h-w_0)=0 \quad [4]$$

Then rearranging and simplifying yields 3-D full Reynolds equation:

$$\frac{\partial}{\partial x}\left[\frac{h^3}{12\eta}\frac{\partial p}{\partial x}\right]+\frac{\partial}{\partial y}\left[\frac{h^3}{12\eta}\frac{\partial p}{\partial y}\right]=\frac{U}{2}\frac{dh}{dx}+\frac{V}{2}\frac{dh}{dy}+(w_h-w_0) \quad [4]$$

$$\frac{1}{12}\left[\frac{\partial}{\partial x}\left(\frac{h^3}{\eta}\frac{\partial p}{\partial x}\right)+\frac{\partial}{\partial y}\left(\frac{h^3}{\eta}\frac{\partial p}{\partial y}\right)\right]=\frac{1}{2}\left[\frac{Udh}{dx}+\frac{Vdh}{dy}\right]+(w_h-w_0) \quad [4]$$

$$\frac{\partial}{\partial x}\left(\frac{h^3}{\eta}\frac{\partial p}{\partial x}\right)+\frac{\partial}{\partial y}\left(\frac{h^3}{\eta}\frac{\partial p}{\partial y}\right)=6\left(\frac{Udh}{dx}+\frac{Vdh}{dy}\right)+12(w_h-w_0) \quad \text{----------(Eq:3.24)} \quad [4]$$

4. MATHEMATICAL MODELING AND DISCRETIZATION

4.1 ELROD ALGORITHM

The Elrod cavitation model reformulates the Reynolds equation by developing a unique differential equation, applicable in both the full lubricant film and the cavitation region by formulating the problem in terms of a new variable (different from pressure) which helps to avoid the tedious calculation of the cavitation boundary and its reformulation [27]. The Elrod algorithm also preserves mass conservation within the entire flow domain.

With the advent of the digital computer, more complex numerical analysis in bearing lubrication became practical. Elrod and Adams [28] proposed an algorithm employing a switch function to handle both the full-film and cavitated regions with a pseudo-compressibility concept; finite difference computation of the one-dimensional problem was furnished to illustrate the method [27]. In 1981, Elrod [24] added a refinement to the Elrod-Adams algorithm, featuring the ADI technique for time-domain with two dimensional simulation of rupture in the bearing film. The latter version is now known as the Elrod cavitation algorithm [27].

The cavitation algorithm presented by Elrod gained worldwide recognition. A few researchers made use of the method to solve specific problems, others tailored the technique, some did further ahead by addition of other theories, and some used the basic concept as a building block for their own algorithm; e.g. Bayada [29] , Bayada et al. [30], Woods and Brewe [31], Vijayaraghavan and Keith [26], Kumar and Booker [32], Claro, Miranda [33], Yu and Keith [34] – and the roster is still increasing.

Although Elrod algorithm is widely accepted but it is deficient to explain morphology of rupture region as it does not treats the Olsson equation for the ruptured region [27]. However, Elrod cavitation algorithm employs a single governing equation for both the full film and partial-film zones [27]**.** A new binary switch function ‘g’ was used with has enabled the pressure terms enabling different fluid behavior in both full film and

cavitation regions [27]. The two-dimensional Reynolds elliptical equation for the full-film region with g set to 1 is with Poiseuille flow terms in the 'x' (circumferential) and 'z' (axial) directions alongwith Couette flow, wedging and squeeze film terms resulting an elliptic equation.

$$"\frac{\partial \rho h}{\partial t}+\frac{\partial}{\partial x}\left(\frac{\rho h U}{2}-g\frac{\rho h^3 U}{12\mu}\frac{\partial p}{\partial x}\right)+\frac{\partial}{\partial z}\left(-g\frac{\rho h^3}{12\mu}\frac{\partial p}{\partial z}\right)=0" \text{ ----------(Eq:4.1) [27]}$$

where x is the circumferential direction, z is the axial direction, t is time, p is pressure, h is the film thickness, ρ is fluid density, U is the rotating journal surface speed, h is the film thickness and μ is the viscosity. In the cavitation region, g is set to 0, resulting in a hyperbolic equation with squeeze & wedging terms:

$$"\frac{\partial \rho h}{\partial t}+\frac{\partial}{\partial x}\left(\frac{\rho h U}{2}\right)=0" \text{----------(Eq:4.2) [27]}$$

In place of pressure p, Equation (4.1) is arranged to solve for a single state variable Θ, which has a dual meaning. The relationship between p and Θ is given by

$$"\Theta=\exp^{\left(\frac{p-p_0}{g\beta}\right)}" \text{----------(Eq:4.3) [27]}$$

where p_0 is the supply pressure (considered ambient here) and β is the bulk modulus introduced as a pseudo-compressibility effect [27]. In the full-film region, Θ is a ratio of densities at each point (actual over cavitated) and in the cavitated region it is the fractional film content (0 is empty and 1 is full of liquid). The adhered film thickness can be obtained from Θ according to

$$"H_a=\Theta H" \text{----------(Eq:4.4) [27]}$$

$$"\Theta=\frac{\rho}{\rho_c}" \text{----------(Eq:4.5) [27]}$$

In the cavitated region, Θ it is the fractional film content (0 is empty and 1 is full of liquid) [27]

"$\Theta = \frac{H_a}{H}$" ----------(Eq:4.6) [27]

Dimensionless Bulk Modulus ‘B’ is given by

"$B = \frac{\beta C^2}{\mu U R}$" ----------(Eq:4.7) [27]

In full film region

“ $g = 1, P > P_c$ ”

In cavitation region

"$g = 0, P = P_c$"

4.2 FINITE DIFFERENCING

Using non-dimensional variables, Equation (4.1) can be written in conservative form as given below:

$$"\frac{\partial E}{\partial T}+\frac{\partial F}{\partial X}+\frac{\partial G}{\partial Z}=0"$$ ----------(Eq:4.8) [27]

$$"E=H\Theta"$$ ----------(Eq:4.9) [27]

$$"F=a_{10}\Theta+a_{11}\frac{\partial \Theta}{\partial X}"$$ ----------(Eq:4.10) [27]

$$"G=a_{22}\frac{\partial \Theta}{\partial Z}"$$ ----------(Eq:4.11) [27]

$$"a_{10}=\frac{H}{4\pi}"$$ ----------(Eq:4.12) [27]

$$"a_{11}=\frac{-B}{48\pi^2}H^3g"$$ ----------(Eq:4.13) [27]

$$"a_{22}=\frac{-B}{48\left(L/D\right)^2}H^3g"$$ ----------(Eq:4.14) [27]

Where ‘H’ is the non-dimensional film thickness which is ratio of film thickness to clearance of bore/bush diameter of journal bearing, ‘B’ is the non-dimensional bulk modulus which is the “lubricants resistance to compression”, or “the measure of elasticity of the fluid”, or “the ratio of differential pressure applied at all surfaces to the strain of fluid”, and ‘L/B’ is the bearing length to diameter ratio.

For the solution of full film region when switch function ‘g’ is set as ‘1’, the finite difference equation of modified Reynolds equation with Elrod algorithm (eq 4.1) takes the form of elliptic equation which is solved with central differencing. And for cavitated region when switch function ‘g’ is set as ‘zero’, the finite difference equation of modified Reynolds equation with Elrod algorithm (eq 4.2) takes the form of hyperbolic equation which is solved with an upwind differencing, so the

conservative form of modified Reynolds equation with Elrod algorithm (eq 4.8) becomes

$$
\begin{aligned}
&"\frac{\left(\Theta^{n+1}-\Theta^{n}\right)}{\Delta T}H_i+\frac{-1}{8\pi\Delta X}\left[g_{i+\frac{1}{2}}E_{i+1}+\left(2-g_{i+\frac{1}{2}}-g_{i-\frac{1}{2}}\right)E_i+\left(2-g_{i-\frac{1}{2}}\right)E_{i-1}\right]\\
&+\frac{-1}{8\pi\Delta X}\left[\left(1-g_{i+\frac{1}{2}}\right)E_i-\left(2-g_{i+\frac{1}{2}}-g_{i-\frac{1}{2}}\right)E_{i-1}+\left(1-g_{i-\frac{1}{2}}\right)E_{i-2}\right]\\
&=\frac{B}{48\pi^2\Delta X^2}\left[H^3_{i+\frac{1}{2}}g_{i+1}\left(\Theta_{i+1}-1\right)-\left(H^3_{i+\frac{1}{2}}+H^3_{i-\frac{1}{2}}\right)g_i\left(\Theta_i-1\right)+H^3{}_{i-\frac{1}{2}}g_{i-1}\left(\Theta_{i-1}-1\right)\right]\\
&+\frac{B}{48\left(L/D\right)^2\Delta Z^2}\left[H^3_{j+\frac{1}{2}}g_{j+1}\left(\Theta_{j+1}-1\right)-\left(H^3_{j+\frac{1}{2}}+H^3_{j-\frac{1}{2}}\right)g_j\left(\Theta_j-1\right)+H^3{}_{j-\frac{1}{2}}g_{j-1}\left(\Theta_{j-1}-1\right)\right]"
\end{aligned}
$$

----------(Eq:4.15) [27]

Solving for Rows Explicitly

$$
\begin{aligned}
&"\left[\frac{\Delta T}{8\pi H_i\Delta X}\left(2-g_{i-\frac{1}{2}}\right)H_{i-1}+\frac{B\Delta T}{48\pi^2H_i\Delta X^2}\left(H^3_{i-\frac{1}{2}}g_{i-1}\right)\right]\Theta_{i-1}\\
&+\left[\begin{array}{l}\omega+\frac{\Delta T}{8\pi H_i\Delta X}\left(2-g_{i+\frac{1}{2}}-g_{i-\frac{1}{2}}\right)H+\frac{B\Delta T}{48\pi^2H_i\Delta X^2}\left(H^3_{i+\frac{1}{2}}+H^3_{i-\frac{1}{2}}\right)g_i+\\ \frac{B\Delta T}{48\left(L/D\right)^2H_i\Delta Z^2}\left(H^3_{j+\frac{1}{2}}+H^3_{j-\frac{1}{2}}\right)g_i\end{array}\right]\Theta_i\\
&+\left[\frac{\Delta T}{8\pi H_i\Delta X}\left(g_{i+\frac{1}{2}}H_{i+1}\right)+\frac{-B\Delta T}{48\pi^2H_i\Delta X^2}\left(H^3_{i+\frac{1}{2}}g_{i+1}\right)\right]\Theta_{i+1}\\
&=\left[\frac{B\Delta T}{48\left(L/D\right)^2H_i\Delta Z^2}\left(H^3_{j-\frac{1}{2}}g_{i-1}\right)\right]\Theta_{j+1}+\left[\omega+\frac{-\Delta T}{48\pi H_i\Delta X}\left(1-g_{i+\frac{1}{2}}\right)H_i\right]\Theta_i\\
&+\left[\frac{B\Delta T}{48\left(L/D\right)^2H_i\Delta Z^2}\left(H^3_{j+\frac{1}{2}}g_{j+1}\right)\right]\Theta_{j+1}\\
&+\left[\frac{-\Delta T}{8\pi H_i\Delta X}\left(1-g_{i-\frac{1}{2}}\right)H_{i-2}\right]\Theta_{i+2}+\left[+\frac{\Delta T}{8\pi H_i\Delta X}\left(2-g_{i+\frac{1}{2}}-g_{i-\frac{1}{2}}\right)H_{i-1}\right]\Theta_{i-1}\\
&+\frac{-B\Delta T}{48\pi^2H_i\Delta X^2}\left(H^3_{i+\frac{1}{2}}g_{i+1}\right)+\frac{B\Delta T}{48\pi^2H_i\Delta X^2}\left(H^3_{i+\frac{1}{2}}+H^3_{i-\frac{1}{2}}\right)g_i+\frac{-B\Delta T}{48\pi^2H_i\Delta X^2}\left(H^3_{i-\frac{1}{2}}g_{i-1}\right)\\
&+\frac{-B\Delta T}{48\left(L/D\right)^2H_i\Delta Z^2}\left(H^3_{j-\frac{1}{2}}g_{j+1}\right)+\frac{B\Delta T}{48\left(L/D\right)^2H_i\Delta Z^2}\left(H^3_{j+\frac{1}{2}}+H^3_{j-\frac{1}{2}}\right)g_j+\frac{-B\Delta T}{48\left(L/D\right)^2H_i\Delta Z^2}\left(H^3_{j-\frac{1}{2}}g_{j-1}\right)"
\end{aligned}
$$

----------(Eq:4.16) [27]

Tri-diagonal coefficients for solving rows:

$$"a_1 = \frac{\Delta T}{8\pi H_i \Delta X}"$$ ----------(Eq:4.17) [27]

$$"a_2 = \frac{B\Delta T}{48\pi^2 H_i \Delta X^2}"$$ ----------(Eq:4.18) [27]

$$"a_3 = \frac{B\Delta T}{48\left(L/D\right)^2 H_i \Delta Z^2}"$$ ----------(Eq:4.19) [27]

$$B_0 = \omega + a_1\left(2 - g_{i+1/2} - g_{i-1/2}\right)H + a_2\left(H^3_{i+1/2} + H^3_{i-1/2}\right)g_i + a_3\left(H^3_{j+1/2} + H^3_{j-1/2}\right)g_j$$

----------(Eq:4.20) [27]

$$"B_1 = a_1\left(g_{i+1/2}H_{i+1}\right) + a_2\left(H^3_{i+1/2}g_{i+1}\right)"$$ ----------(Eq:4.21) [27]

$$"B_2 = a_1\left(2 - g_{i-1/2}\right)H_{i-1} + a_2\left(H^3_{i-1/2}g_{i-1}\right)"$$ ----------(Eq:4.22) [27]

$$"b_5\_\exp = a_3 H^3_{j-1/2}g_{j-1}"$$ ----------(Eq:4.23) [27]

$$"b_0\_\exp = \omega - a_1\left(1 - g_{i+1/2}\right)H_i"$$ ----------(Eq:4.24) [27]

$$"b_4\_\exp = a_3\left(H^3_{j+1/2}g_{j+1}\right)"$$ ----------(Eq:4.25) [27]

$$"b_2\_\exp = a_1\left(2 - g_{i+1/2} + g_{i-1/2}\right)H_{i-1}"$$ ----------(Eq:4.26) [27]

$$"b_3\_\exp = -a_1\left(1 - g_{i-1/2}\right)H_{i-2}"$$ ----------(Eq:4.27) [27]

$$"RHS_{const} = a_2\left[\left(-H^3_{i+1/2}g_{i+1}\right)+\left(H^3_{i+1/2}+H^3_{i-1/2}\right)g_i-\left(H^3_{i-1/2}g_{i-1}\right)\right] + a_3\left[\left(-H^3_{j+1/2}g_{j+1}\right)+\left(H^3_{j+1/2}+H^3_{j-1/2}\right)g_j-\left(H^3_{j-1/2}g_{j-1}\right)\right]"$$ ------(Eq:4.28) [27]

Solving for columns explicitly

$$"\left[\frac{-B\Delta T}{48\left(L/D\right)^2 H_i^2}\left(H^3_{j-1/2}g_{j-1}\right)\right]\Theta_{j-1} + \left[\begin{array}{l}\omega+\frac{\Delta T}{8\pi H_i\Delta X}\left(2-g_{i+1/2}-g_{i-1/2}\right)H_i+\frac{B\Delta T}{48\pi^2 H_i\Delta X^2}\left(H^3_{i+1/2}+H^3_{i-1/2}\right)g_i \\ +\frac{B\Delta T}{48\left(L/D\right)^2 H_i\Delta Z^2}\left(H^3_{j+1/2}+H^3_{j-1/2}\right)g_i\end{array}\right]\Theta_i + \left[\frac{-B\Delta T}{48\left(L/D\right)^2 H_i\Delta Z^2}\left(H^3_{j+1/2}g_{j+1}\right)\right]\Theta_{j+1} = \left[\frac{-\Delta T}{8\pi H_i\Delta X}\left(1-g_{i-1/2}H_{i-2}\right)\right]\Theta_{i-2} + \left[\begin{array}{l}\frac{-\Delta T}{8\pi H_i\Delta X}\left(2-g_{i-1/2}\right)H_{i-1}+\frac{\Delta T}{8\pi H_i\Delta X^2}\left(2-g_{i+1/2/}-g_{i-1/2/}\right)H_{i-1} \\ +\frac{B\Delta T}{48\pi^2 H_i\Delta X^2}\left(H^3_{i-1/2}g_{i-1}\right)\end{array}\right]\Theta_i + \left[\omega+\frac{\Delta T}{8\pi H_i\Delta X}\left(1-g_{i+1/2}\right)H_i\right]\Theta_i + \left[\frac{-\Delta T}{8\pi H_i\Delta X}\left(g_{i+1/2}H_{i+1}\right)+\frac{B\Delta T}{48\pi^2 H_i\Delta X^2}\left(H^3_{i+1/2}g_{i+1}\right)\right]\Theta_{i+1} + \frac{-B\Delta T}{48\pi^2 H_i\Delta X^2}\left(H^3_{i+1/2}g_{i+1}\right)+\frac{B\Delta T}{48\pi^2 H_i\Delta X^2}\left(H^3_{i+1/2}+H^3_{i-1/2}\right)g_i+\frac{-B\Delta T}{48\pi^2 H_i\Delta X^2}\left(H^3_{i-1/2}g_{i-1}\right) + \frac{-B\Delta T}{48\left(L/D\right)^2 H_i\Delta Z^2}\left(H^3_{j-1/2}g_{j+1}\right)+\frac{B\Delta T}{48\left(L/D\right)^2 H_i\Delta Z^2}\left(H^3_{j+1/2}+H^3_{j-1/2}\right)g_j+\frac{-B\Delta T}{48\left(L/D\right)^2 H_i\Delta Z^2}\left(H^3_{j-1/2}g_{j-1}\right)"$$

----------(Eq:4.29) [27]

Tri-diagonal coefficients for solving columns:

$$"a_1 = \frac{\Delta T}{8\pi H_i\Delta X}"$$ ----------(Eq:4.30) [27]

$$"a_2 = \frac{B\Delta T}{48\pi^2 H_i\Delta X^2}"$$ ----------(Eq:4.31) [27]

$$"a_3 = \frac{B\Delta T}{48\left(L/D\right)^2 H_i \Delta Z^2}"$$ ----------(Eq:4.32) [27]

$$"B_5 = -a_3\left(H^3_{j-1/2} g_{j-1}\right)"$$ ----------(Eq:4.33) [27]

$$"B_0 = \omega + a_1\left(2 - g_{i+1/2} - g_{i-1/2}\right)H + a_2\left(H^3_{i+1/2} + H^3_{i-1/2}\right)g_i + a_3\left(H^3_{j+1/2} + H^3_{j-1/2}\right)g_j"$$

----------(Eq:4.34) [27]

$$"B_4 = -a_3\left(H^3_{j+1/2} g_{j+1}\right)"$$ ----------(Eq:4.35) [27]

$$"b_0\_\exp = \omega + a_1\left(2 - g_{i+1/2} - g_{i-1/2}\right)H_i + a_2\left(H^3_{i+1/2} + H^3_{i-1/2}\right)g_i + a_3\left(H^3_{j+1/2} + H^3_{j-1/2}\right)g_j"$$

----------(Eq:4.36) [27]

$$"b_1\_\exp = -a_1\left(g_{i+1/2} H_{i+1}\right) + a_2\left(H^3_{i+1/2} g_{i+1}\right)"$$ ----------(Eq:4.37) [27]

$$"b_2\_\exp = -a_1\left(2 - g_{i-1/2}\right)H_{i-1} + a_2\left(2 - g_{i+1/2} - g_{i-1/2}\right)H_{i-1} + a_3\left(H^3_{i-1/2}\right)g_{i-1}"$$

----------(Eq:4.38) [27]

$$"b_3\_\exp = -a_1\left(1 - g_{i-1/2}\right)H_{i-2}"$$ ----------(Eq:4.39) [27]

$$"RHS_{const} = a_2\left[\left(-H^3_{i+1/2} g_{i+1}\right) + \left(H^3_{i+1/2} + H^3_{i-1/2}\right)g_i - \left(H^3_{i-1/2} g_{i-1}\right)\right]$$
$$+ a_3\left[\left(-H^3_{j+1/2} g_{j+1}\right) + \left(H^3_{j+1/2} + H^3_{j-1/2}\right)g_j - \left(H^3_{j-1/2} g_{j-1}\right)\right]"$$

----------(Eq:4.40) [27]

5. NUMERICAL COMPUTATION

5.1 PROGRAMMING USING ADI TECHNIQUE

An unconditionally stable Alternate Direction Implicit (ADI) technique was used at the governing equation in non-dimensional discretized form as shown at equation: 4.15 which marches in time and reach a steady state solution. Rows and columns were solved as per computational molecule discussed at figure: 5-1 implicitly one by one by making use of tri-diagonal matrix. Coefficients of tri-diagonal matrix were calculated using Jacobi iteration method explicitly. Following is an overview of the ADI procedure [27]:

5.2 ADI PROCEDURE

Figure: 5-1 shows the computational molecule for the tri-diagonal solve. B_1, B_0 and B_2 are used with the solver for solving the rows and B_3 updates the right-hand side explicitly. Then B_5, B_0 and B_4 are used with the tri-diagonal solver for solving the columns. Using the technique of Vijayaraghavan and Keith [26], equation: 4.3 was broken up to preserve balance in time with the ADI scheme, so nearly half of the terms are put into the diagonal solver. The remaining terms are then moved to the right-hand side and taken into account as constants during calculations in one particular direction (either axial sweep or circumferential sweep) [27].

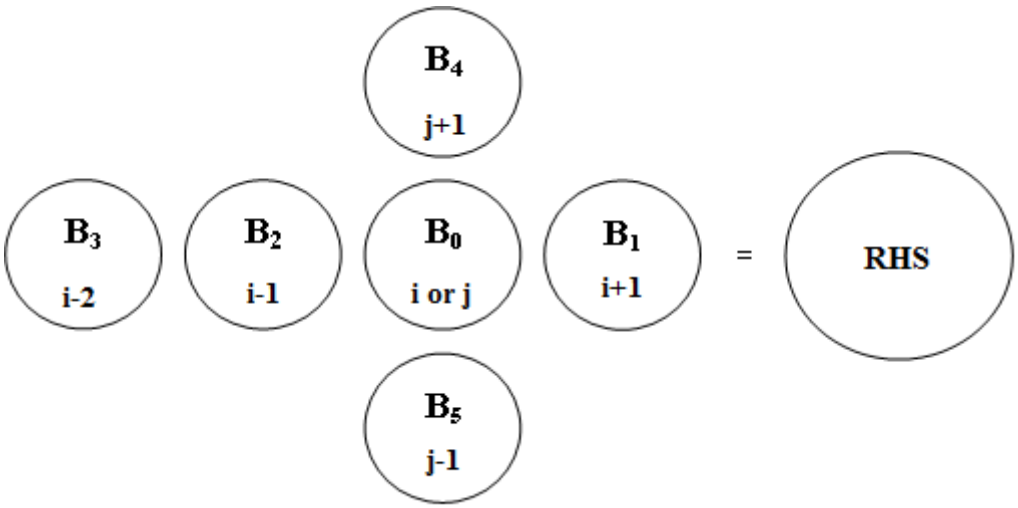

Figure 5-1 : Computational Molecule for ADI Technique (adapted from [27])

5.3 FLOW CHART OF ADI SCHEME

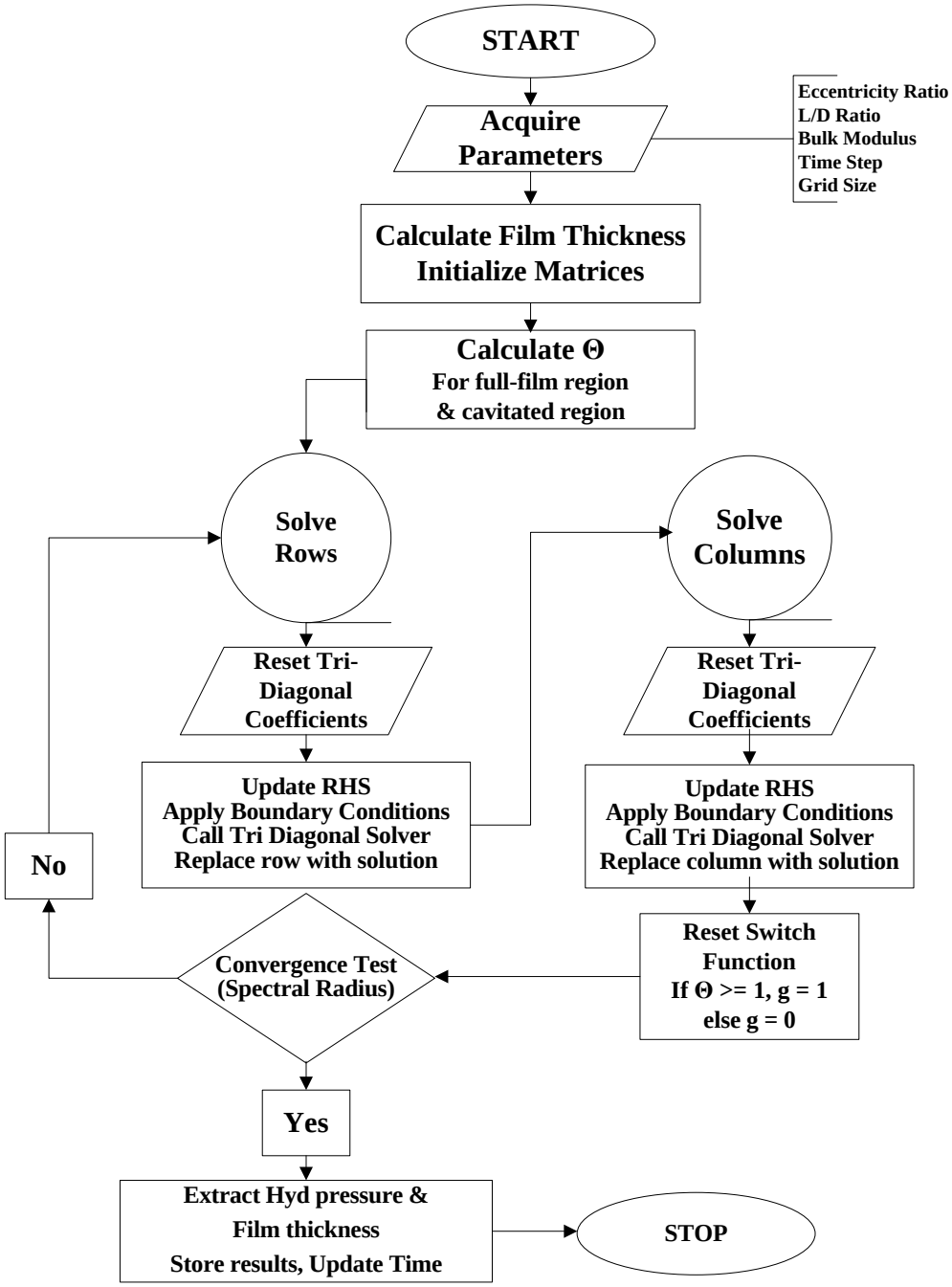

Figure 5-2 : Flow Chart of Algorithm

6. SIMULATION AND ANALYSIS OF RESULTS

The hydrodynamic pressure fields generation between the opposing surfaces of journal and bush walls was simulated on the model developed by solving the modified 2-D, transient, compressible Reynolds equation with Elrod algorithm.

A comprehensive simulation code (see Appendix) was written in Matlab Version 7.12.0.635 (R2011a) for the simple case by using ambient pressure on all four boundaries. Programming details will not be discussed here but we would confine our analysis to the relevant technical details and engineering aspects related to this simulation.

The simulation process involves one complete rotation of shaft i.e. 360 degree. The hydrodynamic pressure fields and corresponding film thickness corresponding to each time step/angle were generated in the simulation.

Through simulations and by taking an insight look at the model, it was revealed that eccentricity ratio and bulk modulus have their pronounced affect for onset of cavitation of lubricant, so our discussions will limit to both parameters.

In order to understand the relative significance of every principal input design parameter it is very essential that we carry out a comprehensive parametric study of cavitation phenomenon of lubricant film in low speed journal bearing. In our existing analysis we have selected three principal input parameters namely, **eccentricity ratio** (ratio of shaft/journal eccentricity to radial clearance between shaft/journal and bush/bore), **speed** of shaft/journal, **radial clearance** between journal/shaft and bush/bore. By going through the mathematical model we can see that the modified Reynolds equation with Elrod's algorithm sums up the effect of speed and radial clearance within a parameter of **dimensionless bulk modulus** by taking into account dimensional bulk modulus of lubricant, viscosity of lubricant and radius of journal/shaft as well (Non-Dimensional Bulk Modulus is the product of Bulk Modulus & Square of Radial Clearance divided by product of Viscosity, Speed & Radius). So we have limited our analysis to the **effect of eccentricity ratio** and **non-dimensional bulk modulus** parameters one by one while keeping values of others as

fixed and then see what effect it will generate on dimensionless lubricant film thickness profile and dimensionless lubricant hydrodynamic pressure profiles.

6.1 EFFECT OF ECCENTRICITY RATIO

Refer to figures: 1-2 & 1-3, **eccentricity ratio** is defined as the ratio of **shaft eccentricity** to the **radial clearance**.

Simulation was run for a mesh size of 24x16, with time step as 0.00001sec, for radial clearance as 50 Microns, for dimensionless bulk modulus as 12000, journal's rotational velocity as 1m/s, lubricant viscosity as 0.05Pa.s for varying eccentricity ratios i.e. 0.01, 0.05, 0.10, 0.15, 0.20, 0.25, 0.30, 0.35, 0.40, 0.45, 0.50, 0.55 and 0.60.

These results were plotted on 3D graphs with x-axis as circumferential length of bearing, z-axis as breadth of bearing and y-axis as dimensionless lubricant hydrodynamic pressure profile & dimensionless lubricant film thickness profile, respectively. The plots were discussed for above mentioned eccentricity ratios in the subsequent section of the dissertation.

6.1.1 Eccentricity Ratio = 0.01

By taking a close examination of the plot for eccentricity ratio as 0.01, it was revealed that dimensionless hydrodynamic pressure profile of lubricant has a very sharp slope and dimensionless film thickness profile was almost uniform and at ratio one throughout the bearing circumference. This case of eccentricity of shaft at near zero i.e. perfectly aligned shaft with hole was studied for simulation purpose only as practically this was the ideal case and it never happens due to the limitations of shaft to hole fits on the basis of either of shaft or hole base(s) system of fits & clearance between them.

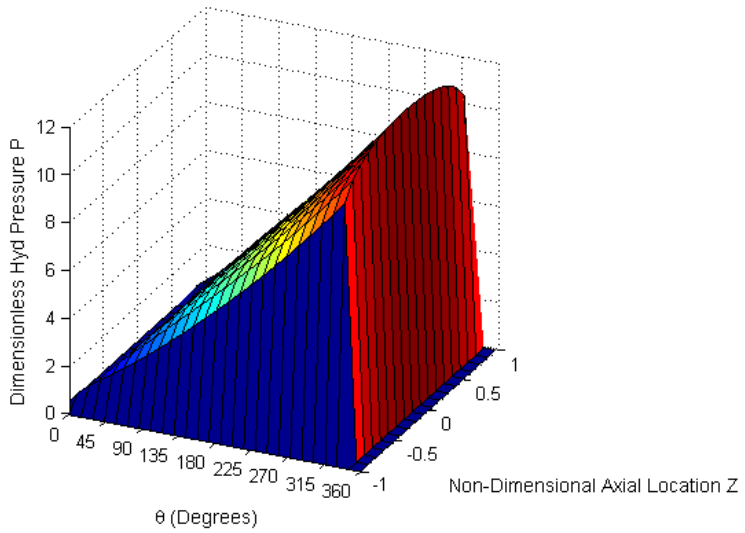

Figure 6-1 : Dimensionless Lubricant Hyd. Pressure Profile for Eccentricity Ratio = 0.01

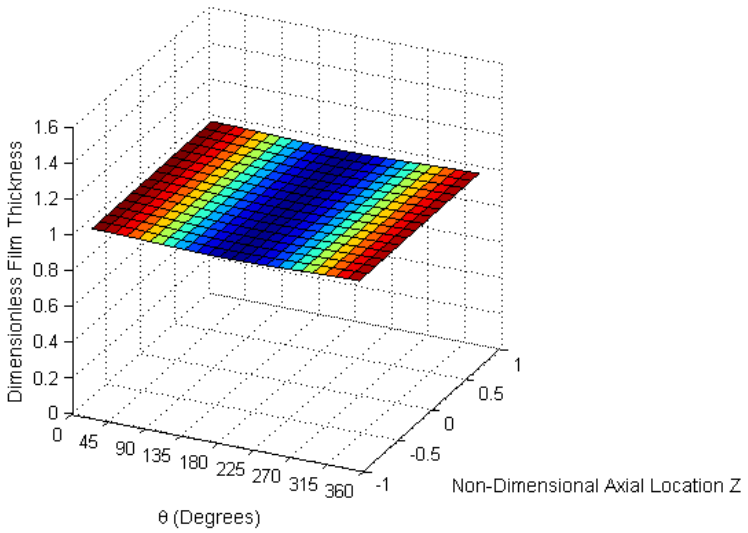

Figure 6-2 : Dimensionless Lubricant Film Thickness Profile for Eccentricity Ratio = 0.01

6.1.2 Eccentricity Ratio = 0.05

By taking a close examination of the plot for eccentricity ratio as 0.05, it was revealed that by increasing eccentricity ratio the sharpness of the slope of lubricant's dimensionless hydrodynamic pressure profile has decreased a bit from the middle of the profile and there was a corresponding dip in lubricant's dimensionless film thickness profile about same angle along the circumference of the bearing. This was the case of very low eccentricity of shaft i.e. nearly aligned shaft with hole.

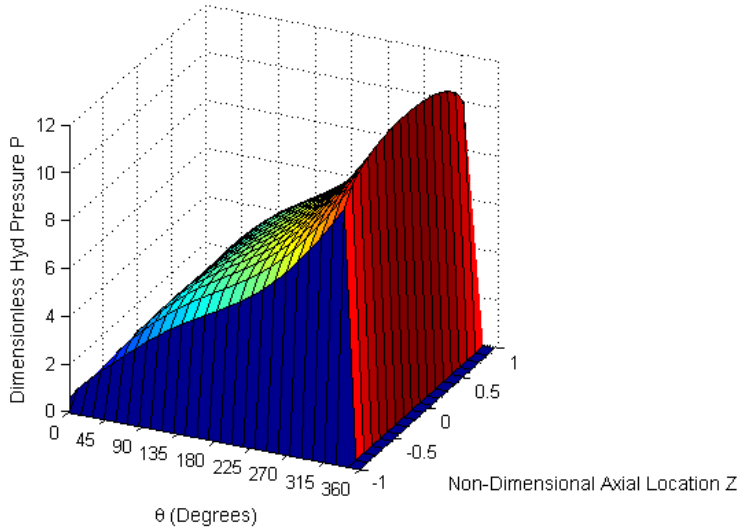

Figure 6-3 : Dimensionless Lubricant Hyd. Pressure Profile for Eccentricity Ratio = 0.05

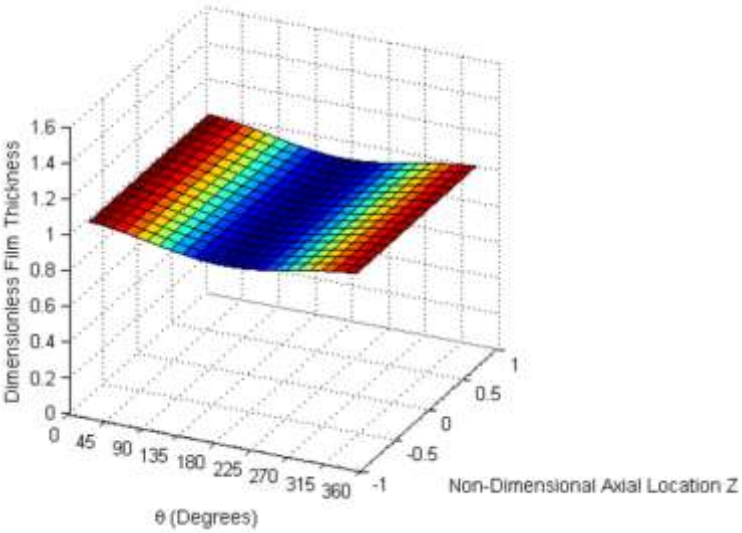

Figure 6-4 : Dimensionless Lubricant Film Thickness Profile for Eccentricity Ratio = 0.05

6.1.3 Eccentricity Ratio = 0.10

By taking a close examination of the plot for eccentricity ratio as 0.10, it was revealed that by increasing eccentricity ratio the sharpness of the slope of lubricant's dimensionless hydrodynamic pressure profile has further decreased from the middle of the profile by a rise in its hydrodynamic pressure from the middle with a drop in maximum hydrodynamic pressure and there was a corresponding further dip in lubricant's dimensionless film thickness profile about the same angle along the circumference of the bearing with a rise from its edges. This was the case of nearly low eccentricity of shaft for a nearly aligned shaft with hole.

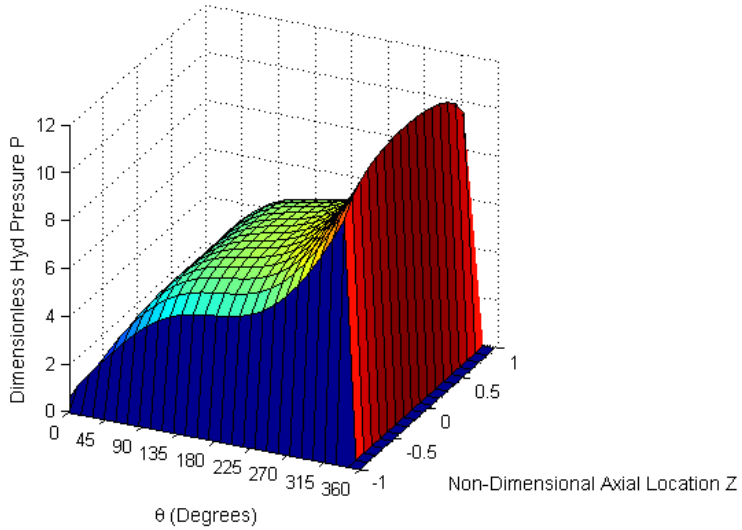

Figure 6-5 : Dimensionless Lubricant Hyd. Pressure Profile for Eccentricity Ratio = 0.10

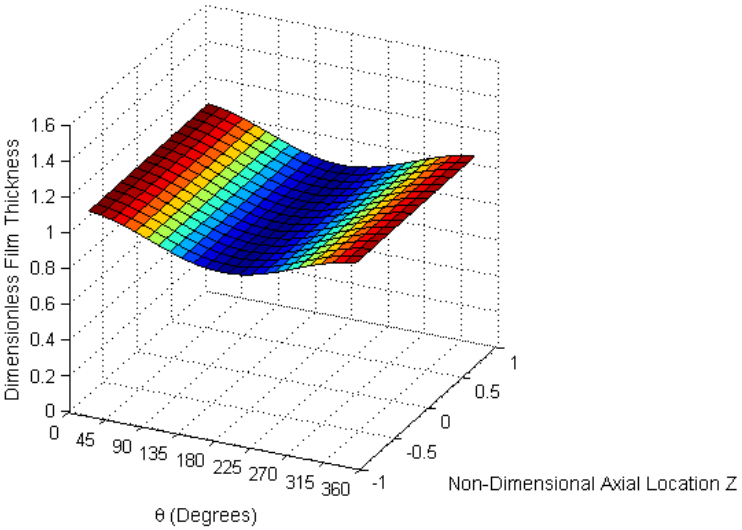

Figure 6-6 : Dimensionless Lubricant Film Thickness Profile for Eccentricity Ratio = 0.10

6.1.4 Eccentricity Ratio = 0.15

By taking a close examination of the plot for eccentricity ratio as 0.15, it was revealed that by increasing eccentricity ratio the sharpness of the slope of lubricant's dimensionless hydrodynamic pressure profile has further decreased from the middle of the profile by a rise in its hydrodynamic pressure from the middle and a rise in pressure from the left half side of the bearing circumference with a drop in maximum hydrodynamic pressure further and there was a corresponding further dip in lubricant's dimensionless film thickness profile about the same angle along the circumference of the bearing with a further rise from its edges.

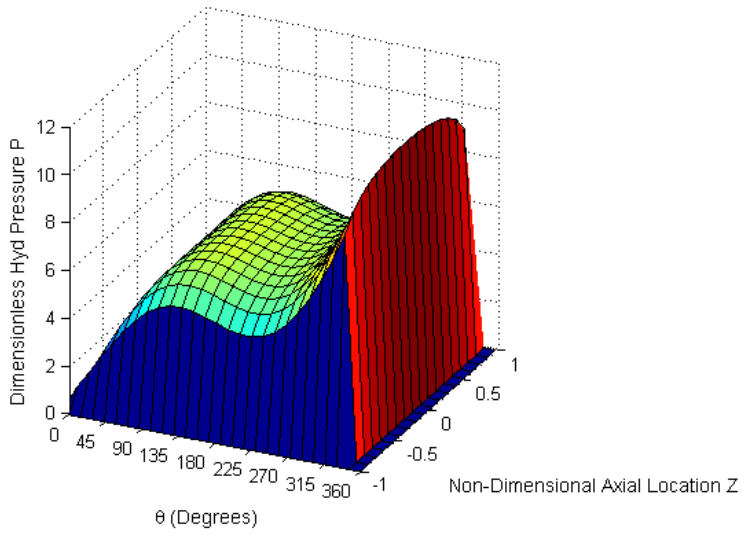

Figure 6-7 : Dimensionless Lubricant Hyd. Pressure Profile for Eccentricity Ratio = 0.15

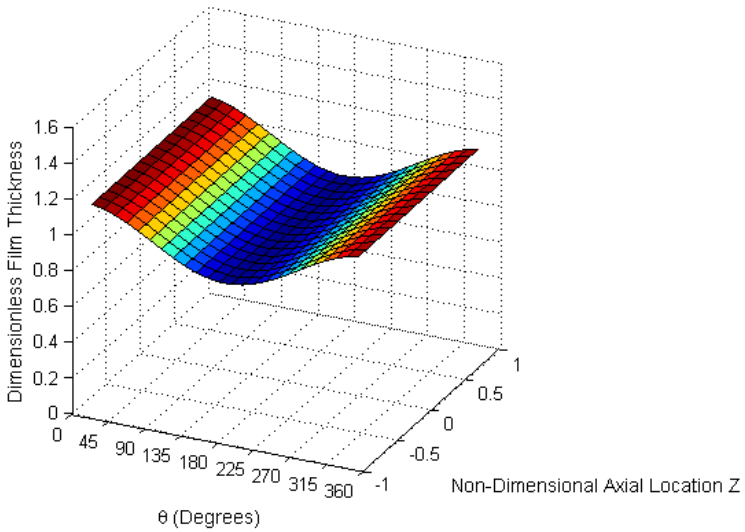

Figure 6-8 : Dimensionless Lubricant Film Thickness Profile for Eccentricity Ratio = 0.15

6.1.5 Eccentricity Ratio = 0.20

By taking a close examination of the plot for eccentricity ratio as 0.20, it was revealed that by increasing eccentricity ratio the previous trend of lubricant's dimensionless hydrodynamic pressure profile and lubricant's dimensionless film thickness profile has changed by rise in all peaks and humps of hydrodynamic pressure profiles alongwith corresponding increase in film thickness profiles about the same angle along the circumference of the bearing with a further rise from its edges and centre and start of a clear converging diverging hydrodynamic film thickness profile.

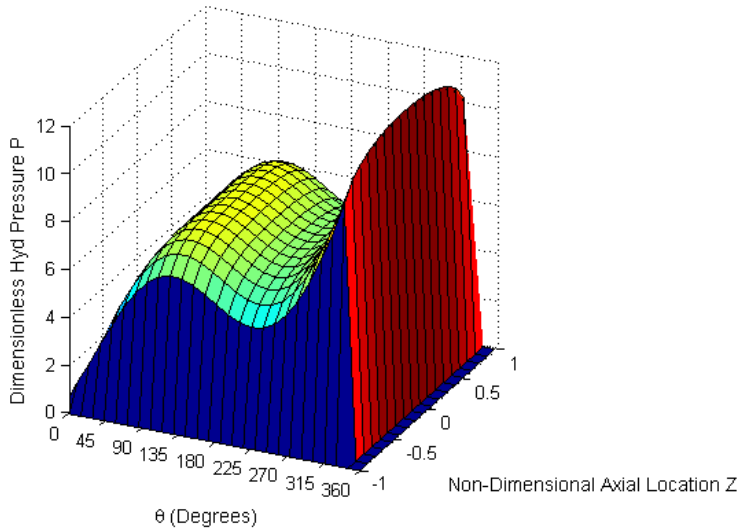

Figure 6-9 : Dimensionless Lubricant Hyd. Pressure Profile for Eccentricity Ratio = 0.20

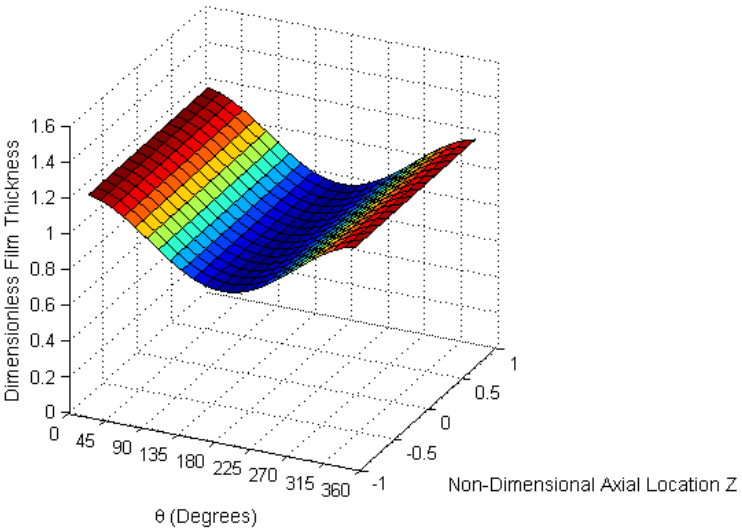

Figure 6-10 : Dimensionless Lubricant Film Thickness Profile for Eccentricity Ratio = 0.20

6.1.6 Eccentricity Ratio = 0.25

By taking a close examination of the plot for eccentricity ratio as 0.25, it was revealed that by increasing eccentricity ratio the peak of the lubricant's dimensionless hydrodynamic pressure profile has increased from left half of the bearing and decreased from the middle and right half of the profile more than as we saw in the case of the eccentricity ratio of 0.15 with a clear sign of converging diverging dimensionless hydrodynamic pressure profile. And lubricant's dimensionless film thickness profile has further risen from its edges with a further drop from the middle along the same angle along the circumference of the bearing.

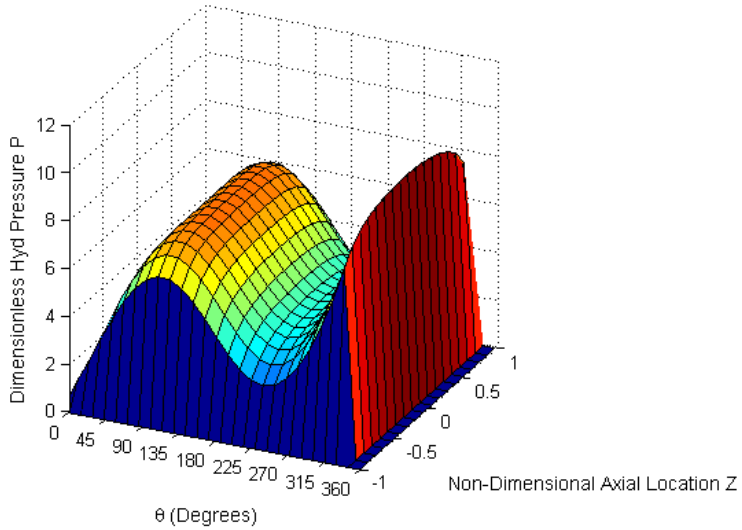

Figure 6-11 : Dimensionless Lubricant Hyd. Pressure Profile for Eccentricity Ratio = 0.25

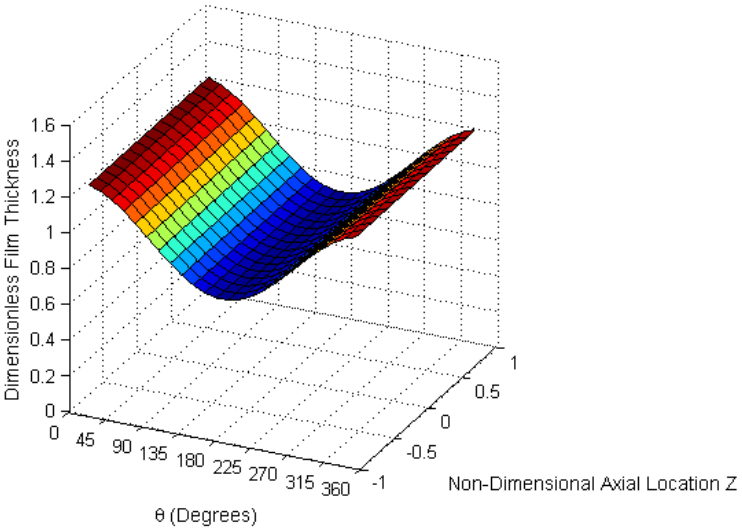

Figure 6-12 : Dimensionless Lubricant Film Thickness Profile for Eccentricity Ratio = 0.25

6.1.7 Eccentricity Ratio = 0.30

By taking a close examination of the plot for eccentricity ratio as 0.30, it was revealed that by increasing eccentricity ratio the peak of the lubricant's dimensionless hydrodynamic pressure profile has dropped from right half of the bearing circumference with a further dip from the middle of the valley within the centre of the peaks and there was a very little change in the peak at left half of the bearing circumference with a more pronounced sign of converging diverging dimensionless hydrodynamic pressure profile. And lubricant's dimensionless film thickness profile has further risen from its edges with a further drop from the middle along the same angle along the circumference of the bearing.

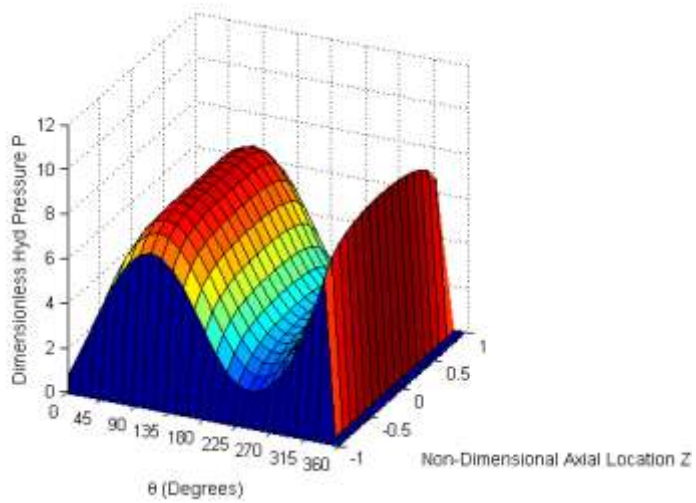

Figure 6-13 : Dimensionless Lubricant Hyd. Pressure Profile for Eccentricity Ratio = 0.30

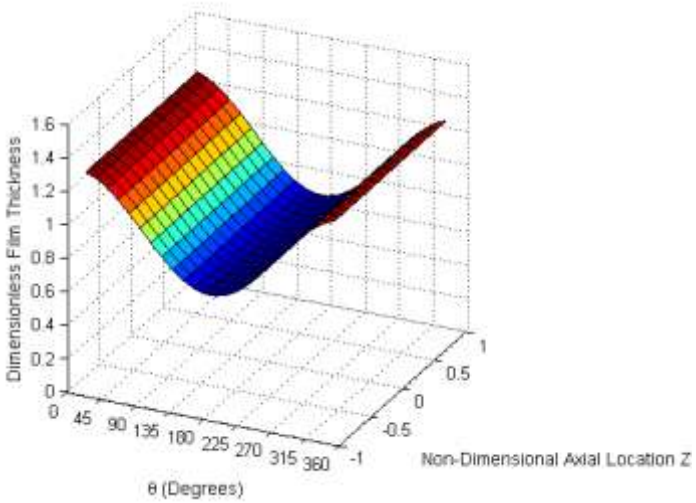

Figure 6-14: Dimensionless Lubricant Film Thickness Profile for Eccentricity Ratio = 0.30

6.1.8 Eccentricity Ratio = 0.35

By taking a close examination of the plot for eccentricity ratio as 0.35, it was revealed that by increasing eccentricity ratio the peak of the lubricant's dimensionless hydrodynamic pressure profile has dropped from right half very sharply along the bearing circumference with a further dip from the middle of the valley in centre of the peaks and there was an appreciable rise in the peak at the left half of the bearing circumference with a an abrupt change of dimensionless hydrodynamic pressure profile. It is due to the fact that this sudden drop of lubricant's hydrodynamic pressure profile from the right half of bearing circumference has made the lubricant pressure to fall below its vapour pressure with the onset of **cavitation** which can be clearly seen from the plot of lubricant's dimensionless film thickness profile at the edges of right half.

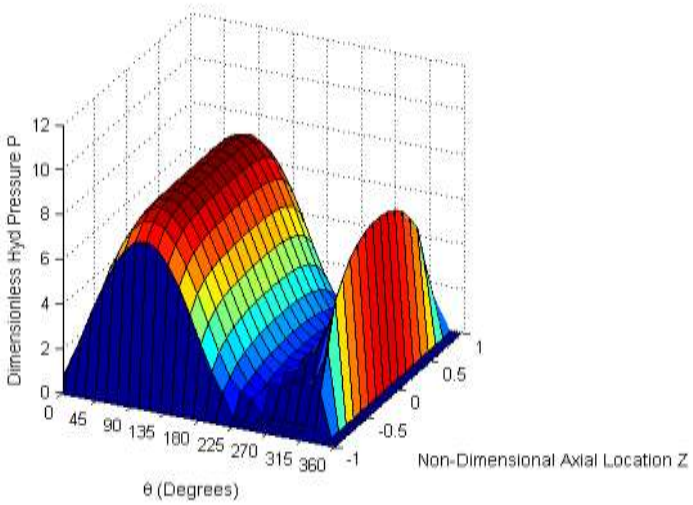

Figure 6-15 : Dimensionless Lubricant Hyd. Pressure Profile for Eccentricity Ratio = 0.35

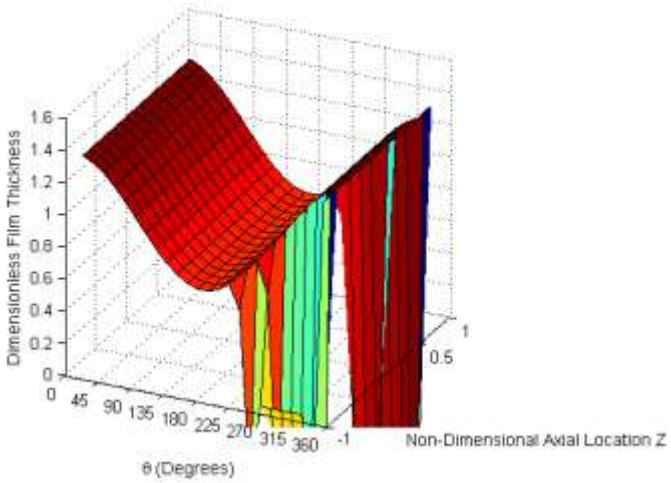

Figure 6-16 : Dimensionless Lubricant Film Thickness Profile for Eccentricity Ratio = 0.35

6.1.9 Eccentricity Ratio = 0.40

By taking a close examination of the plot for eccentricity ratio as 0.40, it was revealed that by increasing eccentricity ratio the peak of the lubricant's dimensionless hydrodynamic pressure profile has now shifted to the left of the bearing circumference and at right side of the bearing circumference hydrodynamic pressure profile of the lubricant has dropped below its vapour pressure further showing a clear sign of **cavitation**. And we could see a corresponding sudden drop of dimensionless lubricant's hydrodynamic film profile from the right half of bearing circumference corresponding to **cavitating** pressures of the lubricant.

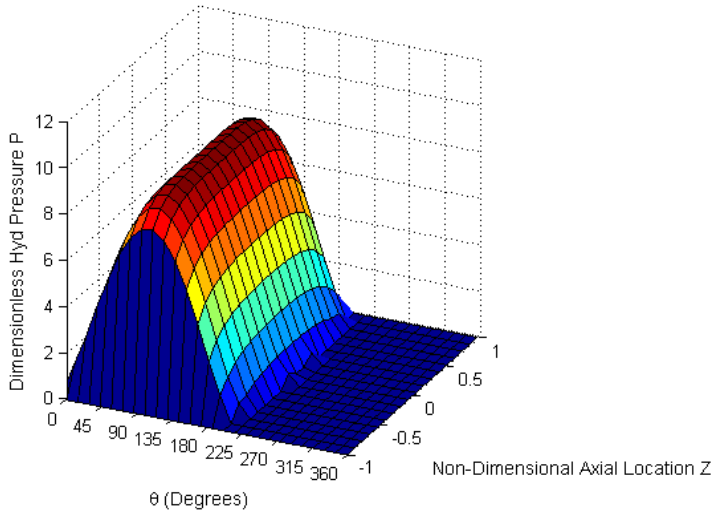

Figure 6-17 : Dimensionless Lubricant Hyd. Pressure Profile for Eccentricity Ratio = 0.40

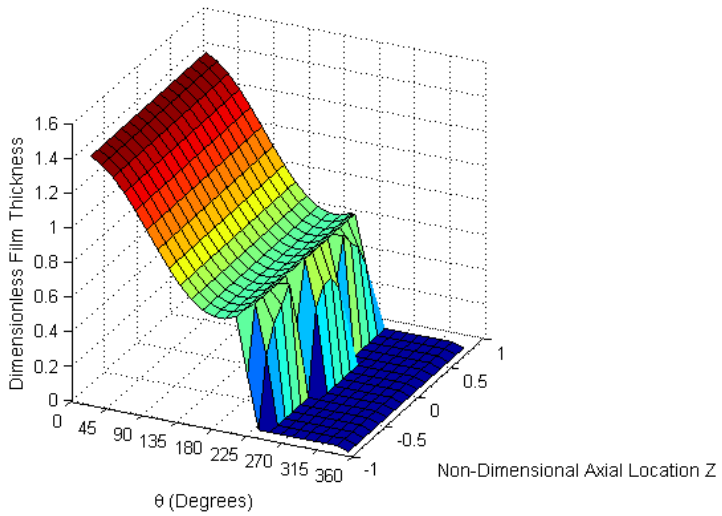

Figure 6-18 : Dimensionless Lubricant Film Thickness Profile for Eccentricity Ratio = 0.40

6.1.10 Eccentricity Ratio = 0.45

By taking a close examination of the plot for eccentricity ratio as 0.45, it was revealed that by increasing eccentricity ratio after the onset of **cavitation** in lubricant pressure the profiles of dimensionless hydrodynamic pressure and dimensionless film thickness are further building up with rise in their peak values at the left side of the bearing circumference and at right side of the bearing circumference we could see a shift towards left in the angle of start of **cavitation** along bearing circumference.

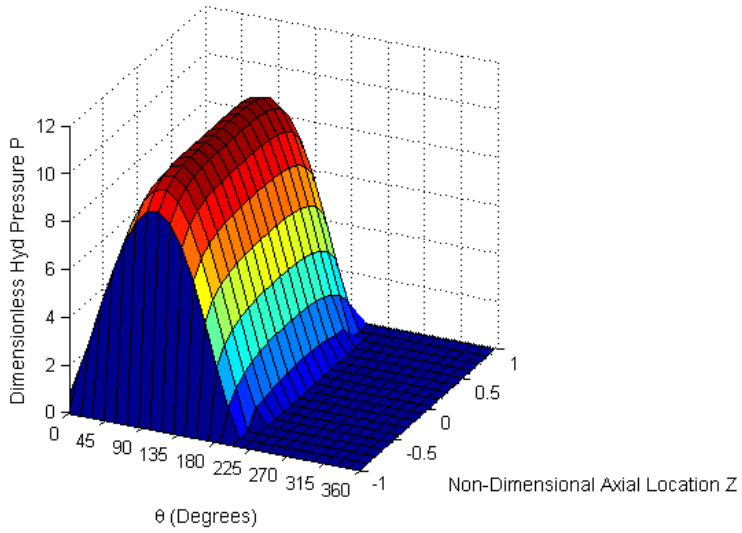

Figure 6-19 : Dimensionless Lubricant Hyd. Pressure Profile for Eccentricity Ratio = 0.45

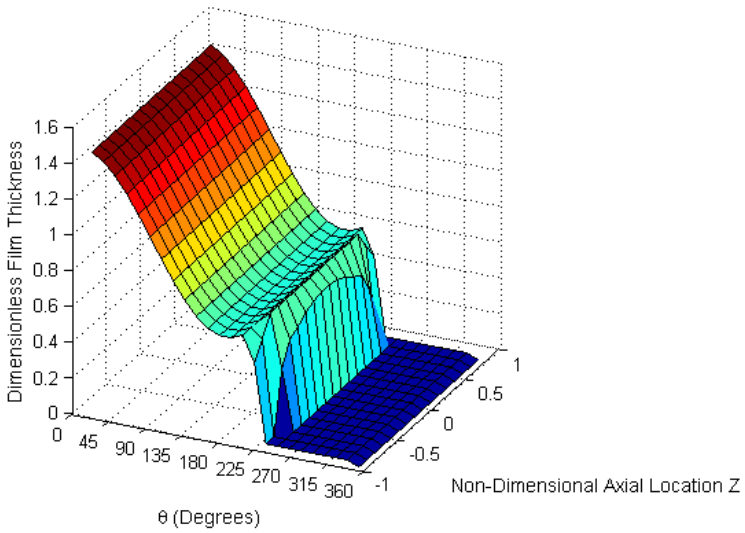

Figure 6-20 : Dimensionless Lubricant Film Thickness Profile for Eccentricity Ratio = 0.45

6.1.11 Eccentricity Ratio = 0.50

By taking a close examination of the plot for eccentricity ratio as 0.50, it was revealed that by increasing eccentricity ratio after the onset of **cavitation** in lubricant pressure the profiles of dimensionless hydrodynamic pressure and dimensionless film thickness are further building up with rise in their peak values at the left side of the bearing circumference. And at the right side of the bearing circumference we could see a further shift towards the left in the angle of the start of **cavitation** along the bearing circumference.

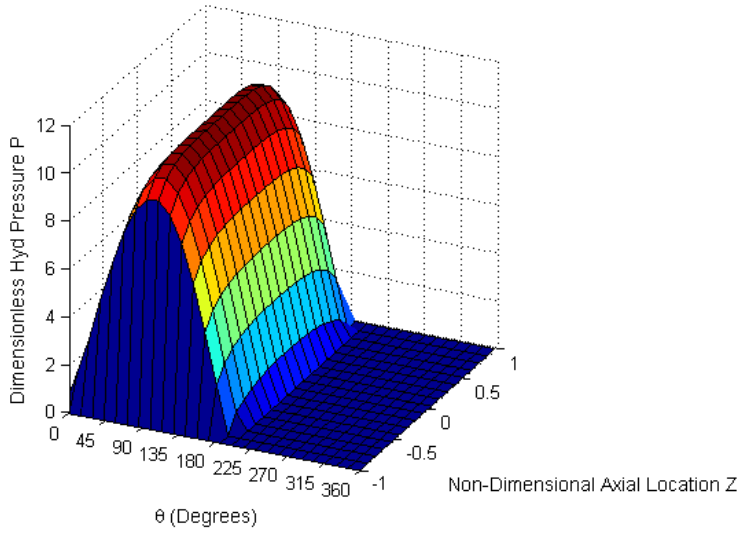

Figure 6-21 : Dimensionless Lubricant Hyd. Pressure Profile for Eccentricity Ratio = 0.50

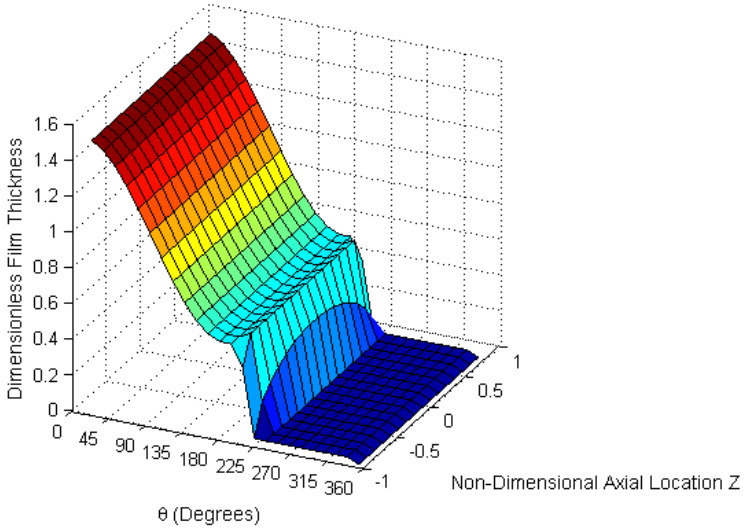

Figure 6-22 : Dimensionless Lubricant Film Thickness Profile for Eccentricity Ratio = 0.50

6.1.12 Eccentricity Ratio = 0.55

By taking a close examination of the plot for eccentricity ratio as 0.55, it was revealed that by increasing eccentricity ratio after the onset of **cavitation** in lubricant pressure the profiles of dimensionless hydrodynamic pressure and dimensionless film thickness are further building up with rise in their peak values at the left side of the bearing circumference. And at the right side of the bearing circumference we could see a further shift towards the left in the angle of the start of **cavitation** along the bearing circumference.

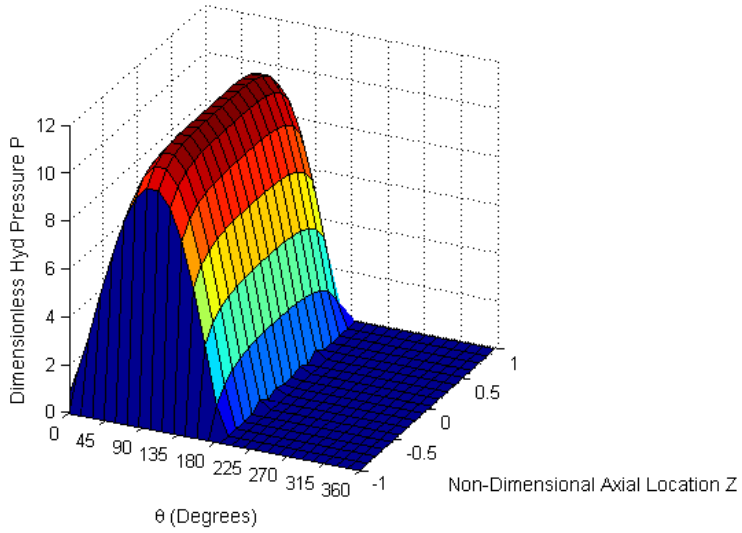

Figure 6-23 : Dimensionless Lubricant Hyd. Pressure Profile for Eccentricity Ratio = 0.55

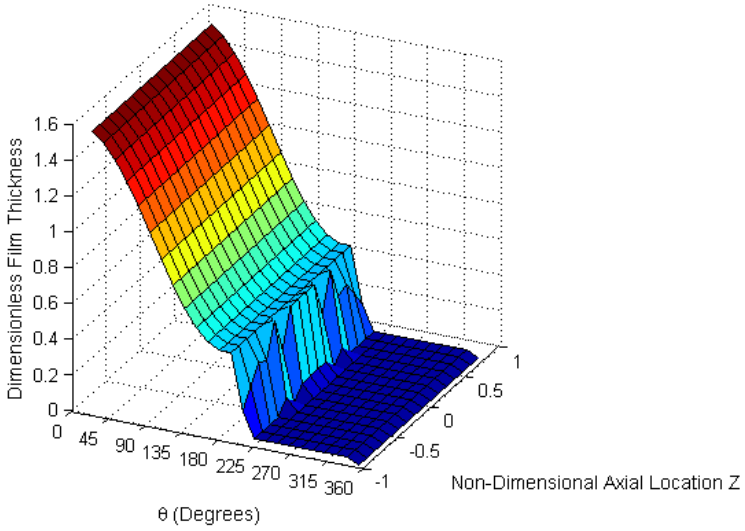

Figure 6-24 : Dimensionless Lubricant Film Thickness Profile for Eccentricity Ratio = 0.55

6.1.13 Eccentricity Ratio = 0.60

By taking a close examination of the plot for eccentricity ratio as 0.60, it was revealed by increasing eccentricity ratio after the onset of **cavitation** in lubricant pressure the profiles of dimensionless hydrodynamic pressure and dimensionless film thickness were further building up with a rise in their peak values at the left side of the bearing circumference. And at the right side of the bearing circumference we could see a further shift towards the left in the angle of the start of **cavitation** along the bearing circumference.

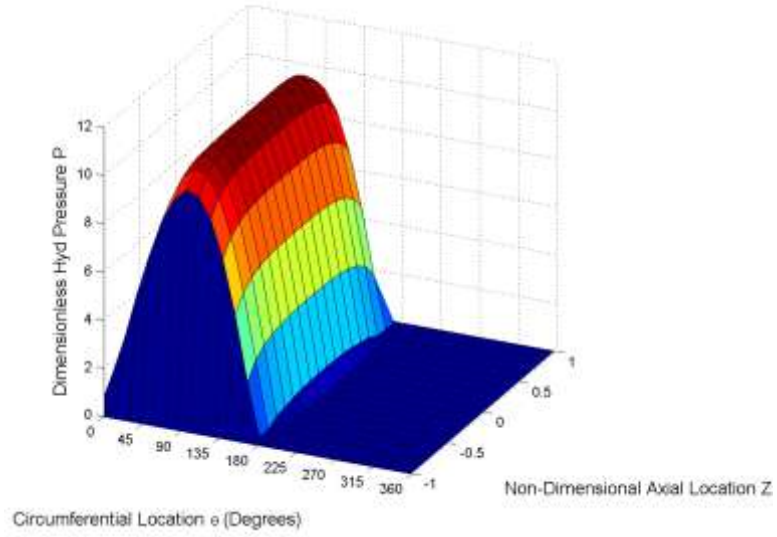

Figure 6-25 : Dimensionless Lubricant Hyd. Pressure Profile for Eccentricity Ratio = 0.60

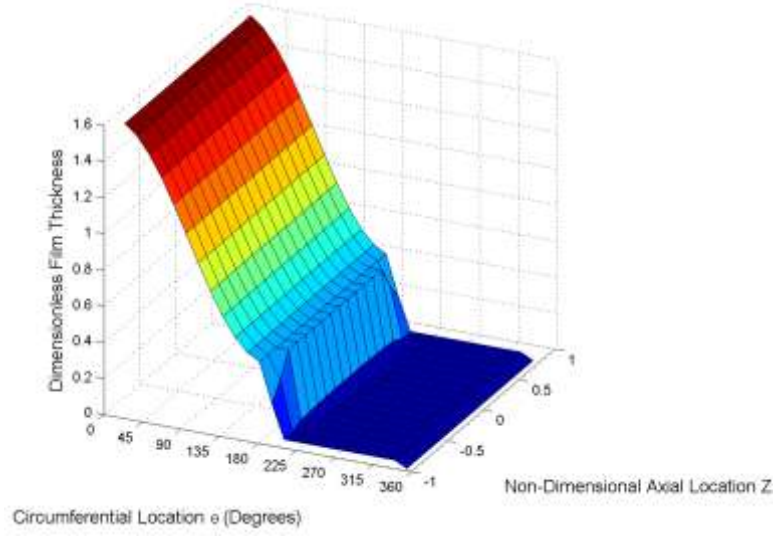

Figure 6-26 : Dimensionless Lubricant Film Thickness Profile for Eccentricity Ratio = 0.60

6.2 EFFECT OF DIMENSIONLESS BULK MODULUS

Dimensionless bulk modulus of lubricant is the product of its **Bulk Modulus** & **Square of Radial Clearance** divided by product of Viscosity, **Speed** & Radius of the journal.

Simulation was run for a mesh size of 24x16, with time step as 0.00001sec, for fixed eccentricity ratio as 0.40 and for varying dimensionless bulk modulus as 14000, 13000, 12750 and 12000 by varying the major parameters affecting dimensionless bulk modulus as Radial Clearance and Speed of the journal.

The results were plotted on 3D graphs with x-axis as circumferential length of bearing, z-axis as breadth of bearing and y-axis as dimensionless lubricant hydrodynamic pressure profile & dimensionless lubricant film thickness profile, respectively. The plots were discussed for above mentioned dimensionless bulk modulus in the subsequent section of the dissertation.

6.2.1 Dimensionless Bulk Modulus = 14,000

By taking a close examination of the plot for dimensionless bulk modulus as 14,000, it was revealed that by selecting higher value of dimensionless bulk modulus it should make lubricant less compressible and same could be seen from the plots below, i.e. lubricant's dimensionless hydrodynamic pressure has a significant converging-diverging profile along the bearing circumference and the lubricant's dimensionless film thickness has its corresponding profile with valley at the minimum value to support the higher load carrying capacity of the bearing.

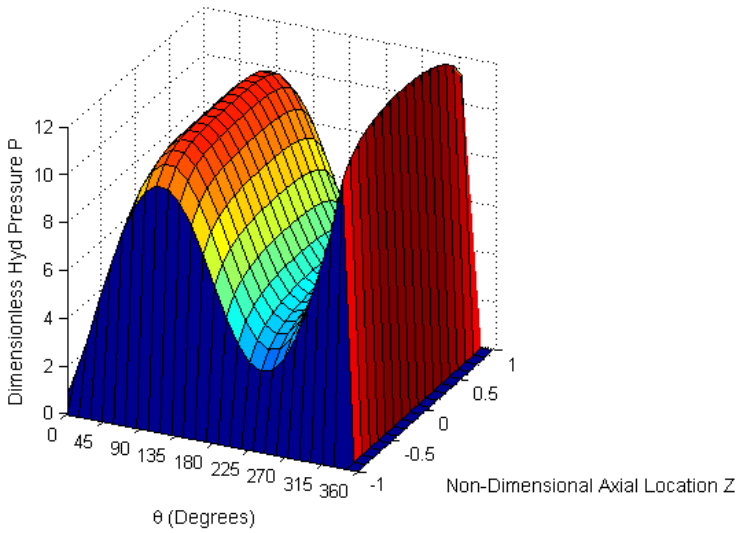

Figure 6-27 : Dimensionless Lubricant Hyd. Pressure Profile for Dimensionless Bulk Modulus = 14,000

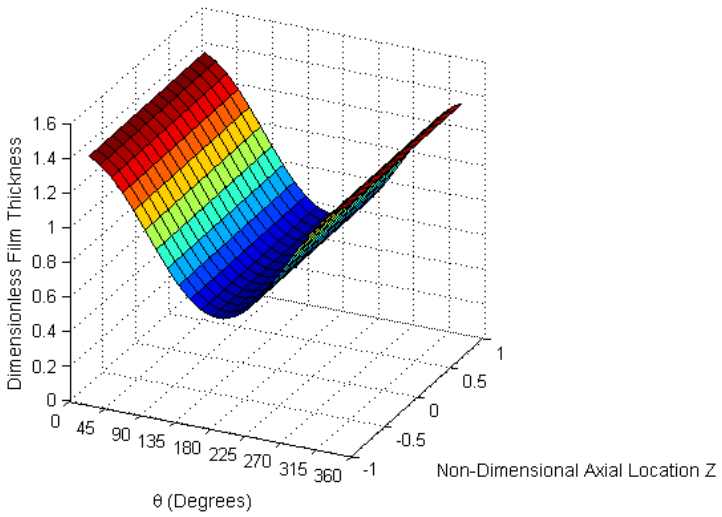

Figure 6-28 : Dimensionless Lubricant Film Thickness Profile for Dimensionless Bulk Modulus = 14,000

6.2.2 Dimensionless Bulk Modulus = 13,000

By taking a close examination of the plot for dimensionless bulk modulus as 13,000, it was revealed that by decreasing dimensionless bulk modulus (either by decreasing the radial clearance or increasing the speed for a fixed viscosity and radius and constant lubricant bulk modulus) from 14,000 to 13,000; both peaks and valley of lubricant's dimensionless hydrodynamic pressure profile have dropped significantly with the similar trend the lubricant's dimensionless film thickness along the bearing circumference with a compromise of load bearing capacity.

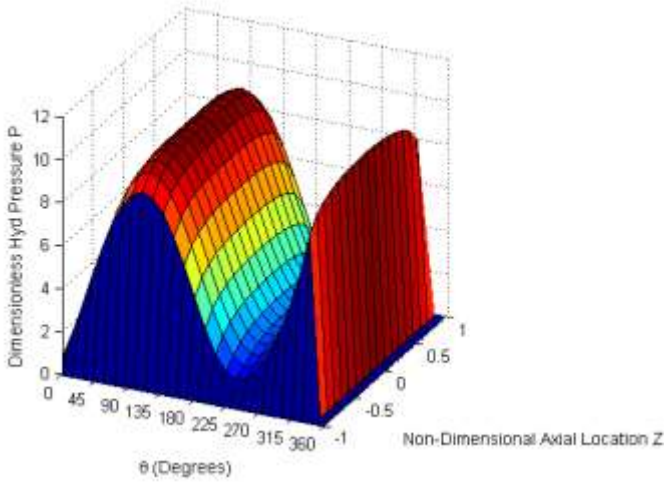

Figure 6-29 : Dimensionless Lubricant Hyd. Pressure Profile for Dimensionless Bulk Modulus = 13,000

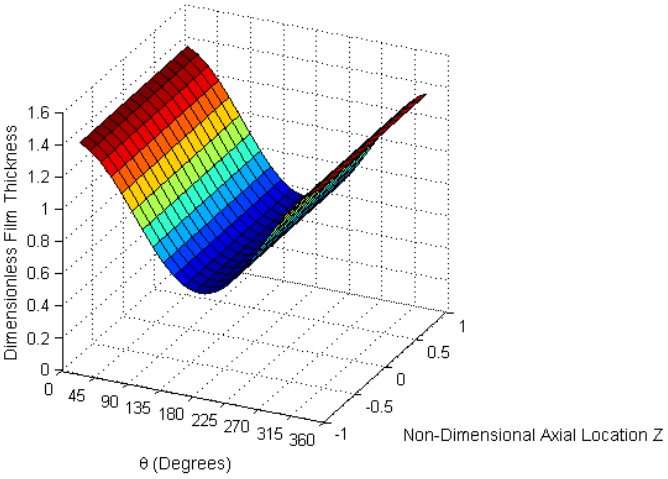

Figure 6-30 : Dimensionless Lubricant Film Thickness Profile for Dimensionless Bulk Modulus = 13,000

6.2.3 Dimensionless Bulk Modulus = 12,750

By taking a close examination of the plot for dimensionless bulk modulus as 12,750, it was revealed that by decreasing dimensionless bulk modulus further (either by decreasing the radial clearance or increasing the speed for a fixed viscosity, radius and constant lubricant bulk modulus) from 13,000 to 12,750; there is a sudden drop in peaks of both left and right alongwith the valley of lubricant's dimensionless hydrodynamic pressure profile. As right peak of lubricant's dimensionless hydrodynamic pressure profile has become too much steeper that lubricant pressure fell below its vapour pressure with the onset of **cavitation** clearly seen at the profile of the lubricant's dimensionless film thickness along the outer edges of the bearing circumference with a compromise of load bearing capacity of bearing.

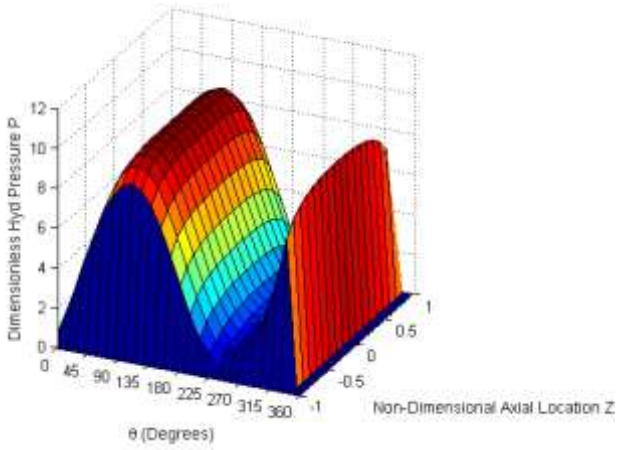

Figure 6-31 : Dimensionless Lubricant Hyd. Pressure Profile for Dimensionless Bulk Modulus = 12,750

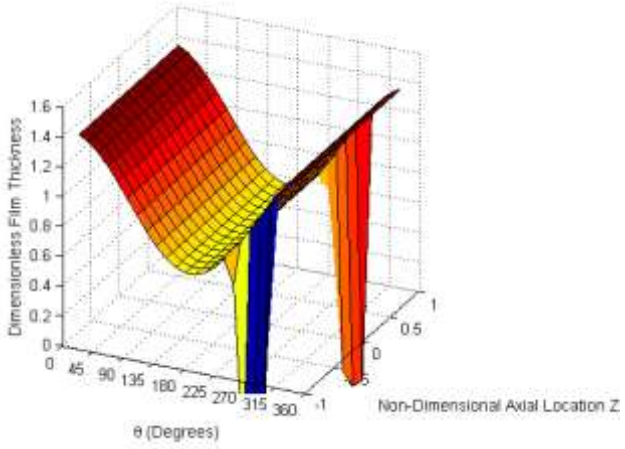

Figure 6-32 : Dimensionless Lubricant Film Thickness Profile for Dimensionless Bulk Modulus = 12,750

6.2.4 Dimensionless Bulk Modulus = 12,000

By taking a close examination of the plot for dimensionless bulk modulus as 12,000, it was revealed that by decreasing dimensionless bulk modulus further (either by decreasing the radial clearance or increasing the speed for a fixed viscosity, radius and constant lubricant bulk modulus) from 12,750 to 12,000; after the onset of **cavitation** in lubricant pressure the profiles of dimensionless hydrodynamic pressure and dimensionless film thickness are further decreasing (unlike as we have seen before in case of eccentricity ratios) with drop in their peak values at the left side of the bearing circumference with further drop in load carrying capacity of bearing. And at right side of the bearing circumference we could see a shift towards left in the angle of start of **cavitation** along bearing circumference.

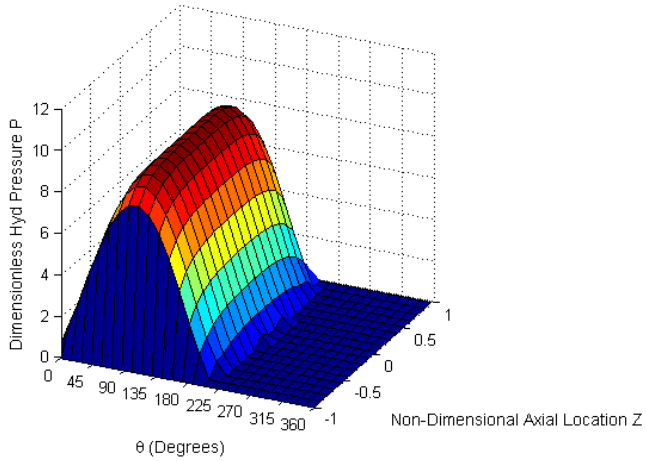

Figure 6-33 Dimensionless Lubricant Hyd. Pressure Profile for Dimensionless Bulk Modulus = 12,000

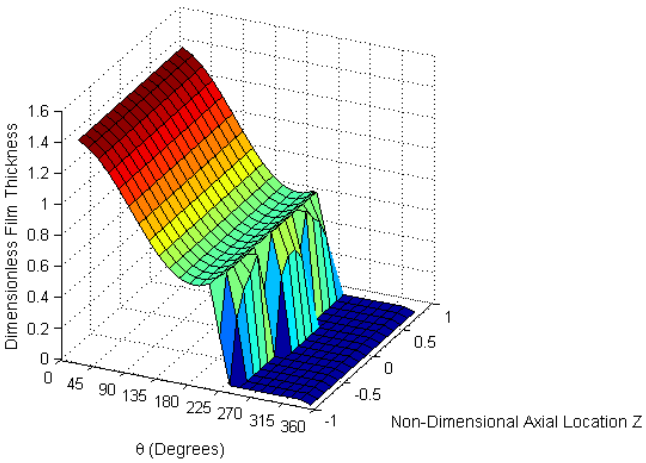

Figure 6-34 : Dimensionless Lubricant Film Thickness Profile for Dimensionless Bulk Modulus = 12,000

7. FINDINGS AND CONCLUSIONS

Following are the findings and conclusions of the research:

- Eccentricity ratio affects the load carrying capacity of bearing significantly
- Eccentricity ratio affects the contact geometry and the dynamics of the bearing
- A disturbed Eccentricity ratio in the journal bearing design may lead to premature journal bearing failure
- Journal's Shaft startup speed invites cavitation and reduced load carrying ability of the bearing and hence must be carefully selected to avoid premature bearing failure
- Radial clearance should not be excessive as it invites unnecessary noise and wear of the journal bearing due to cavitation

8. RECOMMENATIONS FOR FUTURE WORK

Research should be conducted on the following aspects related to cavitation:

- Lubricant Bearing Starvation effects
- Thermal effects on bearing lubrication
- Surface Texturing of bearing surfaces
- Solid Lubricant based Surface Coatings

REFERENCES

1. Berry, J.E. *Oil Whirl and Whip Instabilities- Within Journal Bearings*. 2002.
2. Tower, B., *First Report on Friction Experiments.* Proc. Inst. Mech. Engrs., 1883: p. 632-659.
3. Reynolds, O., *On the Theory of Lubrication and its Application to Mr Beauchamp Tower's Experiments Including an Experimental Determination of the Viscosity of Olive Oil*, in *Philosophical Transactions of the Royal Society of London*1886. p. 157-234.
4. Stachowiak Gwidon W., B.A.W., *Engineering Tribology*. 3rd ed2005: Elsevier.
5. Cameron, A., *Principles of Lubrication*1966: Longmans Green and Co. Ltd., London.
6. *Conference on Tensile Stresses in Oil Films and Bearings*. 1981. London, UK.
7. Young, F.R., *Cavitation*1989: McGraw-Hill New York.
8. Braun, M.J. and W.M. Hannon, *Cavitation formation and modelling for fluid film bearings: a review.* Proceedings of the Institution of Mechanical Engineers, Part J: Journal of Engineering Tribology, 2010. **224**(9): p. 839.
9. Davies, R., *Cavitation in real liquids*, 1964, GM Research Labs, Warren, Michigan.
10. Plesset, M.S., *Bubble dynamics. In Cavitation in real liquids* 1964, GM Research Labs, Warren, Michigan.
11. Westwater, J.W., *Measurements of bubble growth during mass transfer. InCavitation in real liquids (Ed. R.Davies)*, 1964, GM Research Labs, Warren, Michigan; . p. 34–55
12. Prigogine, I., *The molecular theory of surface tension. In Cavitation in real liquids (Ed. R. Davies)*, 1964, GM Research Labs,Warren, Michigan. p. 147-163.
13. Benjamin, T.B., *Surface effects in non-spherical motions of small cavities. In Cavitation in real liquids (Ed. R. Davies)*, 1964, GM Research Labs,Warren, Michigan. p. 164-180.
14. Taylor, G.I., *Cavitation in hydrodynamic lubrication. In Cavitation in real liquids (Ed. R. Davies)*, 1964, GM Research Labs,Warren, Michigan. p. 80-101.
15. Birkhoff, G., *Free boundary problems for viscous flow in channels. In Cavitation in real liquids (Ed. R. Davies)*, 1964, GM Research Labs,Warren, Michigan. p. 102-122.
16. Floberg, L., *Cavitation in lubricating oil films. In Cavitation in real liquids*, 1964, GM Research Labs,Warren, Michigan. p. 138-146.
17. Dowson, D., Godet, M., and Taylor, C. M., *Cavitation and related phenomena in lubrication (Eds D. Dowson, M. Godet, and C. M. Taylor). In Proceedings of the 1st Leeds–Lyon Symposium on Tribology (Eds D. Dowson, M. Godet, and C. M. Taylor)*, 1974, University of Leeds, Leeds, UK. p. 1-238.
18. Brewe, D.E., Ball, J. H., and Khonsari, M. M. , *Introduction. Part 2: current research in cavitating fluid films. In Proceedings of the Cavitation Symposium*, 1988, NASA TM-103184. p. 25–26.
19. Sommerfeld, A., *Zur hydrodynamische theorie der schmiermittelreibung.* Zeit Math. Phys, 1904. **50**: p. 97– 155.
20. Gumbel, L., *Das Problem der Lagerreibung. Mon. Berl. Bezirksverein.* V. D. I., 1914: p. 5, 87–104 and 109-120.

21. Swift, H.W., *The stability of lubricating films in journal bearings.* Proc. Inst. Civil Engnrs London, 1932. **233**: p. 267–288.
22. Stieber, W.D.s., *Hydrodynamische Theorie des Gleitlagers.* V.D.I. Verlag GMBH, Berlin, 1933: p. 106 p.
23. Floberg, L., *On journal bearing lubrication considering the tensile strength of the liquid lubricant.* In Transactions of the Machine Elements Division, Lund Technical University, Lund, Sweden, 1973: p. 1–26.
24. Elrod, H.G., *A cavitation algorithm.* ASME Journal of lubrication technology, 1981. **103**(3): p. 350-354.
25. D. VIJAYARAGHAVAN and T. G. KEITH, J., *Development and Evaluation of a Cavitation Algorithm.* Tribology Transactions, 1989. **32**(2): p. 225-233.
26. Vijayaraghavan, D.a.K., T.G., Jr., *An Efficient, Robust, and Time Accurate Numerical Scheme to a Cavitation Algorithm.* Journal of Lubrication Technology, 1990. **112**: p. 44-51.
27. Bara, R.J., *Rupture Point Movement in Journal Bearings*, 2004, WPI.
28. Elrod, H.G.a.A., M.L., *A Computer Program for Cavitation and Starvation Problems.* Proceedings of the1st Leeds-Lyon Symposium on Tribology, 1975. **Cavitation and Related Phenomena in Lubrication**: p. 37-41.
29. Bayada, G., *Variational Formulation and Associated Algorithm for the Starved Finite Journal Bearing.* Journal of Lubrication Technology, 1983. **105**: p. 453-457.
30. Bayada, G., Chambat, M. and El Alaoui, M., *Variational Formulations and Finite Element Algorithms for Cavitation Problems.* Journal of Tribology, 1990. **112**: p. 398-403.
31. Woods, C.M.a.B., D.E., *The Solution of the Elrod Algorithm for a Dynamically Loaded Journal Bearing Using Multigrid Techniques.* Journal of Lubrication Technology, 1989. **111**: p. 302-308.
32. Kumar, A.a.B., J.F., *A Finite Element Cavitation Algorithm: Application/Validation.* Journal of Tribology, 1991. **113**: p. 255-261.
33. Claro, J.C.P.a.M., A.A.S., *Analysis of Hydrodynamic Journal Bearings Considering Lubricant Supply Conditions.* Proceedings of the Institution of Mechanical. Engineers 1993. **207**: p. 93-101.
34. Yu, Q.a.K., T.G., Jr., *Prediction of Cavitation in Journal Bearings Using a Boundary Element Method.* Journal of Tribology, 1995. **117**: p. 411-421.

APPENDIX

```
% In the name of Allah, The Most Beneficent & The Most Merciful
clc, clear all, close all;
LbyD = 1;
Res = 4;
dt = 0.00001;
BM = 12000;
X = 6 * Res;
Z = round(4 * LbyD * Res);
ecc = 0.35;
Pc = 0.0;
W1 = ([0 360 -LbyD LbyD 0.0 12.0]);
W2 = ([0 360 -LbyD LbyD 0.0 1.6]);
XXT = ([0:45:360]);
YYT = ([-LbyD:LbyD*0.5:LbyD]);
ZZT = ([0:2:12]);
ZZZ = ([0.0:0.2:1.6]);
ecc_str = num2str(round(ecc*10.0));
LbyD_str = num2str(LbyD);
ss_str = num2str(Res);
movie_file = strcat('eps_0', ecc_str,'_', LbyD_str, 'x', ss_str)
movie = avifile(movie_file, 'compression', 'FFDS','fps', 1,
'quality', 100); % output file for movie
dh = zeros(X+3, Z+2);
zh = zeros(X+3, Z+2);
p = zeros(X+3, Z+2);
press = p;
TH_mid = ones(X+3, Z+2);
TH_prev = ones(X+3, Z+2);
sg = ones(X+3, Z+2);
dth = 2.0*pi/(X+1);
dz = 2.0*LbyD/(Z+1);
L_D = dz/dth;
for j = 1:Z+2
for i = 1:X+3
dh(i,j) = dth * (i-2);
zh(i,j) = dz * (j-1) - LbyD;
H(i,j) = 1.0 + ecc * cos(dh(i,j));
end;
end;
for j = 2:Z+1
for i = 3:X+2
theta(i-2,j-1) = dth * (i-2);
zed(i-2,j-1) = dz * (j-1) - LbyD;
Ha(i-2,j-1) = 1.0 + ecc * cos(theta(i-2,j-1));
end;
end;
for j = 2:Z+1
for i = 3:X+2
if i <= (X/2 + 2)
p(i,j) = 20.0;
TH_mid(i,j) = exp(p(i,j)/(sg(i,j)*BM));
p(i,j) = 25.0;
TH_prev(i,j) = exp(p(i,j)/(sg(i,j)*BM));
else
sg(i,j) = 0.0;
TH_mid(i,j) = 0.1;
TH_prev(i,j) = 0.1;
end;
```

```
end;
end;
omega = 0.1; t = 0.0; rho = 1.5;
count = 0; delt_n_prev = 0.1;
k = 1;
t = t + dt;
count = count + 1;
delt_n = 0.0;
% reset tri-diagonal coefficients
clear b0 rhs;
b0 = zeros(1,X);
rhs = zeros(1,X);
% solve for rows explicitly one at a time
for j = 2:Z+1
for i = 3:X+2
a1 = dt/(H(i,j)*8.0*pi*dth);
a2 = BM*dt/(H(i,j)*48.0*pi^2.0*dth^2.0);
a3 = BM*dt/(H(i,j)*48.0*L_D^2.0*dz^2.0);
b2(i-2) = a1*(2.0-0.5*(sg(i,j)+sg(i-1,j)))*H(i-1,j)...
+ a2*(0.5*(H(i,j)+H(i-1,j)))^3.0*sg(i-1,j);
b0(i-2) = omega + a1*(2.0-0.5*(sg(i,j)+sg(i+1,j)))...
-0.5*(sg(i,j)+sg(i-1,j))*H(i,j)+a2*((0.5*(H(i,j)+H(i+1,j)))^3.0...
+(0.5*(H(i,j)+H(i-1,j)))^3.0)*sg(i,j)...
+a3*((0.5*(H(i,j)+H(i,j+1)))^3.0...
+0.5*(H(i,j)+H(i,j-1))^3.0)*sg(i,j);
b1(i-2) = a1*0.5*(sg(i,j)+sg(i+1,j))*H(i+1,j)...
- a2*(0.5*(H(i,j)+H(i+1,j)))^3.0*sg(i+1,j);
b5_exp = a3*(0.5*(H(i,j)+H(i,j-1)))^3.0*sg(i,j-1);
b4_exp = a3*(0.5*(H(i,j)+H(i,j+1)))^3.0*sg(i,j+1);
b0_exp = omega - a1*(1.0-0.5*(sg(i,j)+sg(i+1,j)))*H(i,j);
b3_exp = a1*(2.0-0.5*(sg(i,j)+sg(i+1,j))...
-0.5*(sg(i,j)+sg(i-1,j)))*H(i-1,j);
b2_exp = -a1*(1.0-0.5*(sg(i,j)+sg(i-1,j)))*H(i-2,j);
rhs_const = - a2*( (0.5*(H(i,j)+H(i+1,j)))^3.0*sg(i+1,j)...
- ((0.5*(H(i,j)+H(i+1,j)))^3.0+(0.5*(H(i,j)+H(i-
1,j)))^3.0)*sg(i,j)...
+ (0.5*(H(i,j)+H(i-1,j)))^3.0*sg(i-1,j) )...
- a3*( (0.5*(H(i,j)+H(i,j+1)))^3.0*sg(i,j+1)...
- ((0.5*(H(i,j)+H(i,j+1)))^3.0+(0.5*(H(i,j)+H(i,j-
1)))^3.0)*sg(i,j)...
+ (0.5*(H(i,j)+H(i,j-1)))^3.0*sg(i,j-1) );

rhs(i-2) = rhs_const + (omega + b0_exp)* TH_prev(i,j)...
+ b2_exp*TH_prev(i-1,j) + b3_exp*TH_prev(i-2,j)...
+ b5_exp*TH_prev(i,j-1) + b4_exp*TH_prev(i,j+1);
end;
rhs(1) = rhs(1) - b2(1) * TH_prev(2,j);
tomas(b3, b5, b1, rhs, k, X);
for i = 3:X+2
TH_mid(i,j) = rhs(i-2);
end;
end;
for i = 3:X+2
for j = 2:Z+1
a1 = dt/(H(i,j)*8.0*pi*dth);
a2 = BM*dt/(H(i,j)*48.0*pi^2.0*dth^2.0);
a3 = BM*dt/(H(i,j)*48.0*L_D^2.0*dz^2.0);
b5(j-1) = -a3*(0.5*(H(i,j)+H(i,j-1)))^3.0*sg(i,j-1);
b0(j-1) = omega + a1*(2.0-0.5*(sg(i,j)+sg(i+1,j)))...
-0.5*(sg(i,j)+sg(i-1,j))*H(i,j)...
+a2*((0.5*(H(i,j)+H(i+1,j)))^3.0...
```

```
+(0.5*(H(i,j)+H(i-1,j)))^3.0)*sg(i,j)...
+a3*((0.5*(H(i,j)+H(i,j+1)))^3.0...
+(0.5*(H(i,j)+H(i,j-1)))^3.0)*sg(i,j);
b4(j-1) = -a3*(0.5*(H(i,j)+H(i,j+1)))^3.0*sg(i,j+1);
b3_exp = -a1*(1.0-0.5*(sg(i,j)+sg(i-1,j)))*H(i-2,j);
b2_exp = -a1*(2.0-0.5*(sg(i,j)+sg(i-1,j)))*H(i-1,j)...
+ a2*(2.0-0.5*(sg(i,j)+sg(i+1,j))...
-0.5*(sg(i,j)+sg(i-1,j)))*H(i-1,j)...
+a3*(0.5*(H(i,j)+H(i-1,j)))^3.0*sg(i-1,j);
b0_exp = -a1*(1.0-0.5*(sg(i,j)+sg(i+1,j)))*H(i,j);
b1_exp = -a1*(0.5*(sg(i,j)+sg(i+1,j)))*H(i+1,j)...
- a2*(0.5*(H(i,j)+H(i+1,j)))^3.0*sg(i+1,j);
rhs_const = - a2*( (0.5*(H(i,j)+H(i+1,j)))^3.0*sg(i+1,j)...
- ((0.5*(H(i,j)+H(i+1,j)))^3.0+(0.5*(H(i,j)+H(i-
1,j)))^3.0)*sg(i,j)...
+ (0.5*(H(i,j)+H(i-1,j)))^3.0*sg(i-1,j) )...
- a3*( (0.5*(H(i,j)+H(i,j+1)))^3.0*sg(i,j+1)...
- ((0.5*(H(i,j)+H(i,j+1)))^3.0+(0.5*(H(i,j)+H(i,j-
1)))^3.0)*sg(i,j)...
+ (0.5*(H(i,j)+H(i,j-1)))^3.0*sg(i,j-1) );
rhs(j-1) = b3_exp*TH_mid(i-2,j) + b2_exp*TH_mid(i-1,j)...
+ (omega + b0_exp) * TH_mid(i,j) + b1_exp*TH_mid(i+1,j)...
+ rhs_const;
end;
rhs(1) = rhs(1) - b5(1) * TH_mid(i, 1);
rhs(Z) = rhs(Z) - b4(Z) * TH_mid(i, Z+2);
tomas(b3, b2, b1, rhs, k, Z);
for j = 2:Z+1,
delt_n = delt_n + abs(rhs(j-1) - TH_prev(i,j));
TH_prev(i,j) = rhs(j-1);
end;
end;
for j = 2:Z+1
for i = 3:X+2
if TH_prev(i,j) >= 1.0
sg(i,j) = 1.0;
else
sg(i,j) = 0.0;
end;
end;
end;
rho = delt_n / delt_n_prev;
delt_n_prev = delt_n;
if count > 20
for i = 3:X+2
for j = 2:Z+1
if sg(i,j) < 1
Ha(i-2,j-1) = TH_prev(i,j)*H(i,j);
press(i-1,j) = Pc + 0.0;
else
Ha(i-2,j-1) = H(i,j);
press(i-1,j) = Pc + sg(i,j) * log(TH_prev(i,j));
end;
end;
end;
subplot(2,1,1)
surf(dh*180.0/pi, zh, press)
axis(W1); set(gca,'XTick', XXT, 'YTick', YYT, 'ZTick', ZZT);
view(25.0, 25.0);
mf = getframe(gcf);
movie = addframe(movie,mf);
```

```
end;
count, t
hold on
figure(1)
surf(dh*180.0/pi, zh, press)
axis(W1); set(gca,'XTick', XXT, 'YTick', YYT, 'ZTick', ZZT);
view(25.0, 25.0);
zlabel('Dimensionless Hyd Pressure P',...
'FontSize', 10, 'FontName', 'New Times Roman');
xlabel('Circumferential Location \theta (Degrees)',...
'FontSize', 10, 'FontName', 'New Times Roman');
ylabel('Non-Dimensional Axial Location Z',...
'FontSize', 10, 'FontName', 'New Times Roman');
figure(2)
surf(theta*180.0/pi, zed, Ha)
axis(W2); set(gca,'XTick', XXT, 'YTick', YYT, 'ZTick', ZZZ);
view(25.0, 25.0);
zlabel('Dimensionless Film Thickness',...
'FontSize', 10, 'FontName', 'New Times Roman');
xlabel('Circumferential Location \theta (Degrees)',...
'FontSize', 10, 'FontName', 'New Times Roman');
ylabel('Non-Dimensional Axial Location Z',...
'FontSize', 10, 'FontName', 'New Times Roman');
```